EFFECT OF DIFFERENT PARAMETERS ON THE MICROSTRUCTURE AND PERFORMANCE OF ZIF-8 MEMBRANES

A Thesis

By

GOKULA KRISHNAN RAMU

Submitted to the Office of Graduate and Professional Studies of
Texas A&M University
In partial fulfillment of the requirements for the degree of

MASTER OF SCIENCE

Chair of Committee,	Hae-Kwon Jeong
Committee Members,	Mustafa Akbulut
	Choongho Yu
Head of Department,	Nazmul Karim

December 2016

Major Subject: Chemical Engineering

ABSTRACT

Metal-Organic Frameworks (MOFs) are nanoporous materials comprising of metal nodes coordinated to organic ligands. They exhibit regular crystal lattice structures with well-defined pores. Owing to the ease with which the organic groups can be given different chemical functionalities, MOFs display highly flexible surface chemistry and pore sizes. This makes them suitable for their application as gas separation membranes. Zeolitic-Imidazolate Frameworks (ZIFs), a sub-class of MOFs, have pore sizes in the range of C_3-C_6 hydrocarbons, and in particular ZIF-8 (pore size 3.4Å), can be used for the industrially important propylene/propane separation. Because heterogeneous nucleation and growth of ZIF-8 crystals on the ceramic supports is not favored, their synthesis as membranes is complicated and involves multiple steps. Of the different synthesis techniques, the microwave-assisted seeding followed by the secondary growth is one of the most effective because of strong attachment of seed crystals to the supports achieved. The microstructure, and consequently, performance of membranes grown by this method is highly sensitive to different parameters and a systematic study of some of these will help to identify the best microstructure possible, reduce synthesis time, and improve reproducibility. Some of the parameters studied are different metal salt sources, aging of precursor solutions, post-synthetic activation time and membrane performance under high pressure and temperature.

ZIF-8 seed layers and membranes were synthesized using the same recipe but different zinc salts to investigate the effect of different zinc metal sources on both seed layer and membrane performance and morphology. It was found that ZIF-8

membranes from zinc nitrate based seed layers had the best performance possibly due to better grain boundaries. Zinc nitrate-based ZIF-8 membranes showed good propylene/propane separation performance without any structural degradation when tested under harsher pressure and temperature (~ 7 bar and 100 °C) conditions. Reduction in total synthesis time along with significant improvement in membrane performance was achieved by reducing the post synthesis activation time and using aged precursor solutions.

DEDICATION

To my dad, Ramu

To my mom, Chithra Ramu

To my uncles, Veeraraghavan, Balaji and Chakravarthy

To my aunts, Rohini Veeraraghavan, Vijayalakshmi Balaji and Latha Chakravarthy

To my friends,

ACKNOWLEDGEMENTS

I would first like to thank my Research Advisor and Committee Chair, Dr. Hae-Kwon Jeong, for his continuous support and guidance, both professional and personal, through the course of my research. Next, I would like to thank Dr. Mustafa Akbulut and Dr.Choongho Yu for their support and being a part of my committee.

I would also like to acknowledge the contributions of Dr. Hyuk-Taek Kwon, Moonjoo Lee and all my group members for their tremendous support, encouragement and helping with my experiments.

Special thanks to Amresh Chand, Raja Ramanathan and Harish Kumar for their continuous support and help during the course of my Masters at College Station.

I would also like to thank all my friends, colleagues, and the department faculty and staff (with special thanks to Ashley) for making my time at Texas A&M University a great experience.

Finally, thanks to my parents for their support, encouragement and for believing in me.

NOMENCLATURE

Btu	British Thermal Unit
GC	Gas Chromatograph
HP	High Pressure
HT	High Temperature
mIm	2-methyl imidazole
MOF	Metal-Organic Framework
MW	Microwave
Psi	Pounds per square inch
SEM	Scanning Electron Microscope
XRD	X-ray Diffractometer
ZIF	Zeolitic-Imidazolate Framework
ZnA	Zinc Acetate Dihydrate
ZnC	Zinc Chloride Anhydrous
ZnN	Zinc Nitrate Hexahydrate

TABLE OF CONTENTS

LIST OF FIGURES

LIST OF TABLES

CHAPTER I

INTRODUCTION

1.1 Why Is Gas Separation Essential?

With the rise in global energy consumption, the demand for essential commodities like water, air, fuel, chemicals etc. has been increasing manifold. Separation has an important role to play in the production of these commodities. More specifically, some of the vital products for our day-to-day survival like fuels, plastics, power, etc. are obtained from the processing of different gases like ethylene, propylene and other light hydrocarbons, oxygen, natural gas, etc. These gases often need to be separated from other non-essential gases, making gas separation a growing field over the last several years.

1.2 Advantages of Using Membranes for Gas Separation

There are several competing technologies when it comes to the separation of gases, namely cryogenic distillation, pressure swing adsorption and chemical adsorption [1], [2]. Cryogenic distillation is very similar to normal distillation except that “cryogenic” implies lower temperatures are used for separation. Pressure swing adsorption (PSA) involves pressurizing and adsorbing the gases using common adsorbents like zeolites, silica gel, activated carbon, etc [3]. As the name suggests, chemical adsorption involves adsorbing gases (mainly CO_2) on amine-based adsorbents [4], [5]. The advantages and disadvantages of these technologies [6] have been summarized in a table by a review article [7], which is shown as Table 1.

Table 1: A comparison between gas separation technologies (Adapted from Ref. 7)

Technology	Advantages	Disadvantages
Cryogenic Distillation	Can operate at high pressures with good product purity and recovery	High cost and energy consumption
Absorption	Simple to operate	Low purity and recovery of products
Pressure Swing Adsoprtion	Simple process with very high purity of products	Low pressure operation only

Membranes have many advantages compared to the above conventional gas separation techniques [8], [9]:

- They are more energy-efficient because no phase change is generally involved
- Easier operability because large distillation towers are no longer needed
- More convenient for small-scale separations
- Some membranes have shown reliability even under high pressure (1000 psi) operation [10]
- Cost effective because they do not need expensive adsorbents

For example, for hydrogen recovery from refinery off-gas, it was reported that membranes are more viable than PSA and cryogenic distillation. Membranes consumed only 30% of the energy consumed by cryogenic distillation for hydrogen separation without any loss in purity [11], [12]. With the annual separation energy consumption in the United States being a staggering 4500 trillion Btu, this amounts

to a significant reduction in the separation energy when membranes are used [1], [2]. Prasad et al have evaluated membranes and conventional separation techniques against each other in depth in a nice publication [13].

1.3 Historical Development of Gas Separation Membranes

Having established that membranes are indeed a worthwhile substitute for the conventional methods, a brief timeline for the development of some of the commercially applied gas separation membranes (up to the year 2000) is shown in Fig 1 [8]

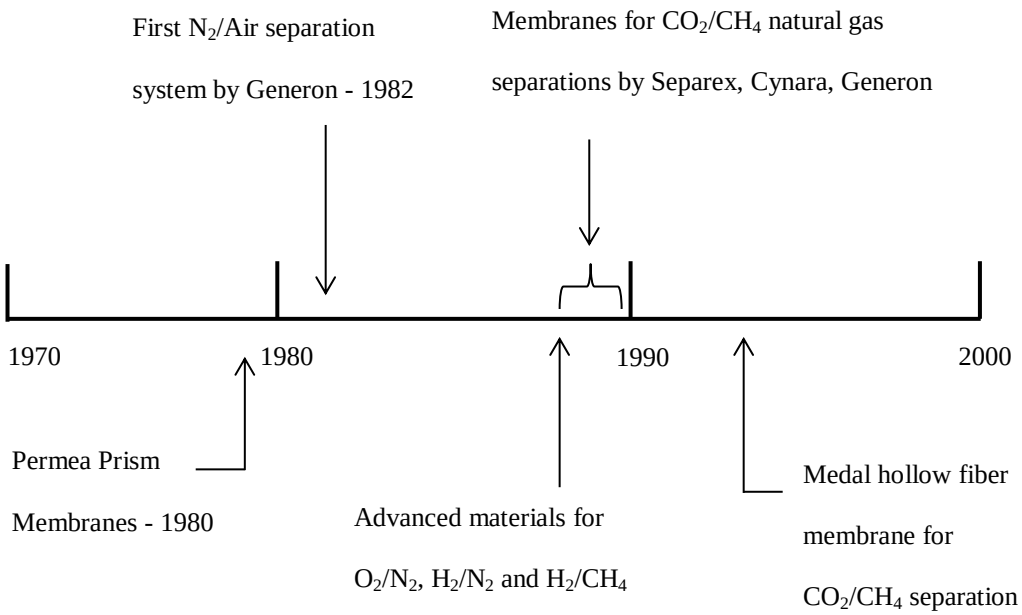

Fig 1: Milestones in the industrial application of membranes (Adapted from Ref. 8)

Table 2 provides a concise account of the main industrial gas separations currently in operation.

Table 2: Main industrial applications of gas separation membranes (Adapted from Ref. 14)

Common Gases	**Process Application**
H_2/N_2	Ammonia purge gas
H_2/CO	Syngas
O_2/N_2	Nitrogen generation and oxygen enrichment
H_2/hydrocarbons	Hydrogen recovery
CO_2/CH_4	Natural gas sweetening
H_2O/CH_4	Natural gas dehydration
H_2S/hydrocarbons	Sour gas treatment
Ethylene/Ethane	Polymer processing
Propylene/Propane	
p-Xylene/o-Xylene	p-Xylene production

1.4 Different Types of Membranes

Some of the emerging gas separations today include carbon capture, paraffin/olefin separation and butane isomer separations. Just as Richard Baker had predicted in his seminal review article on membrane technologies [8], these require the use of a wide variety of membrane materials and types like polymer membranes [15], carbon molecular sieves [16-18], mixed matrix membranes [19], zeolites [20], and facilitated transport membranes [7]. A summary of the different membrane materials and their typical gas separation applications is provided in Table 3.

Table 3: Summary of membrane types and their gas separation applications

Membrane Types	Gas Pairs	Industrial Application	Reference
Polymer	CO_2/CH_4, O_2/N_2, H_2/N_2, H_2/CH_4, H_2/CO, H_2O/Air	Acid gas treatment, nitrogen enrichment, ammonia purge recovery, refinery gas purification, syngas adjustment, and dehydration	1
Carbon molecular sieve	O_2/N_2	Nitrogen enrichment	21,22,23,24, 25,26,27
Mixed matrix	CO_2/CH_4, C_3H_6/C_3H_8	Acid gas treatment, polymerization	28
Zeolites	C_3H_6/N_2	Hydrocarbon enrichment and Polymerization	29
Facilitated transport	CO_2/N_2, CO_2/CH_4	Carbon capture and acid gas treatment	30, 31, 32, 33, 34

The current membrane separation market is dominated by polymer membranes because of their low production costs and ease of synthesis [8]. However, they suffer from several difficulties like lack of chemical stability, highly structure dependent permeability-selectivity trade-off and plasticization issues when operated for olefin/paraffin separations under industrial conditions [1], [8]. While zeolite membranes have excellent chemical and thermal stability, they suffer from a limited range of pore sizes, leading to a lack of process flexibility (Fig 2). Their cost of

production is also very high (in the range of $3000-$4000 per m^2). Mixed matrix membranes present difficulties in effectively dispersing the inorganic zeolite particles in the primary polymer phase [35]. Facilitated transport membranes can be easily affected by impurities while carbon molecular sieves lack structural strength [36].

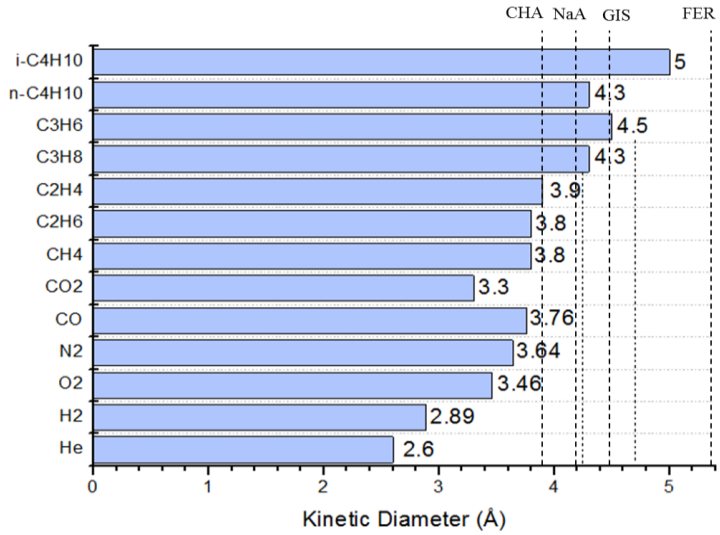

Fig 2: Comparison between zeolite pore sizes and the size of typical gases requiring separation in industry (Adapted from Ref. 37)

1.5 What Are Metal-Organic Frameworks (MOFs)

MOF's are a class of nanomaterials, consisting of a hybrid inorganic-organic structure. The inorganic component, metal nodes are connected to organic linkers (also known as chelating ligands) by strong coordination covalent bonds. Mesoscale to nanoscale pore size distributions are possible with MOF's, making them attractive for separation of gas molecules of all sizes. Control over pore sizes and their properties are achieved by modifying the functional groups of the organic linker molecules chosen for MOF synthesis [38]. Due to these unique properties, chemists

have been focusing their attention on generating and studying the properties of different MOF structures for more than years 15 years now.

1.5.1 Structures

Because MOF chemistry is a relatively new research area, a huge number of MOF structures with different pore sizes, structure, properties have been developed and studied in depth for their application in gas separations [39], gas storage [40], optical devices [41] and as chemical sensors [42]. The crystallographic structures of some of MOF's are shown in Figure 3.

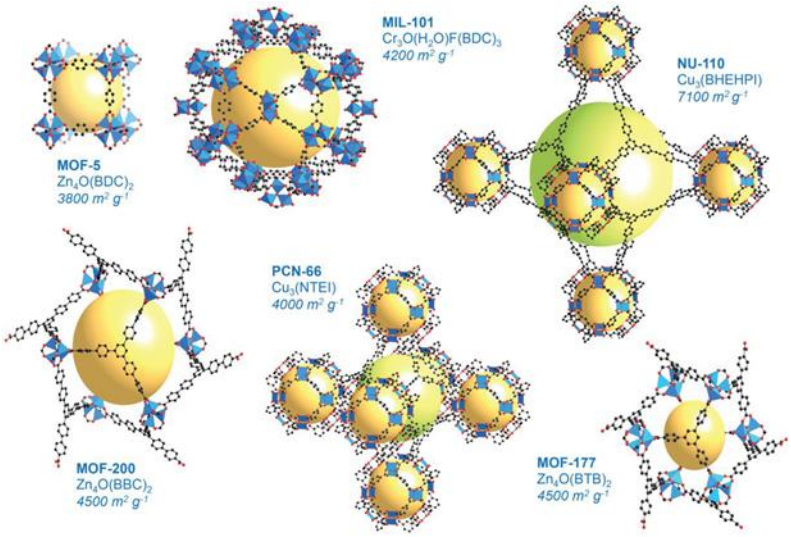

Fig 3: Various MOF structures (from Ref 43)

Zeolitic-Imidazolate Frameworks (ZIF's) are an important sub-class of MOFs which have been recently getting a lot of attention because of their unique advantages suitable for gas separations [44-50]. Similar to other MOF's, ZIF's consist of metal nodes (predominantly zinc or cobalt) connected by different bridging imidazole

ligands. They are called “zeolitic” because of their M-N-M bond angle of 145°, which is very close to the Si-O-Si bond angle in zeolites (Fig 4) [51]. However, unlike zeolites that have very rigid structures with fixed pore sizes, ZIFs exhibit flexible pore sizes due to “gate-opening effect” which arises from the flapping vibrations of the ligand molecule [52], [53]. This in combination with excellent stability make ZIF’s very interesting for separations of light hydrocarbons.

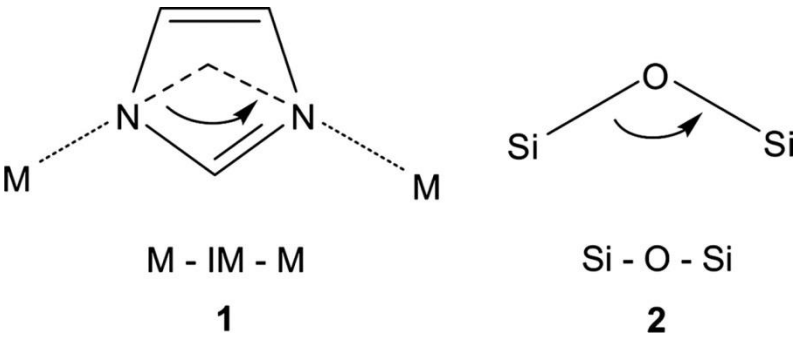

Fig 4: Bond angles in (1) ZIFs and (2) zeolites

1.5.2 Stability of MOFs

The main bonding in MOFs is a coordination bond, which is weaker kinetically than ionic and even covalent bonds. The kinetic stability of the bonds is dependent on the specific coordination bond present in the MOF. A useful rule to understand this kinetic stability order of the coordination bond in MOF’s is the Pearson rule, which states that bonds formed by acids and bases of similar character are most stable. He classified the acids and bases as hard, intermediate and soft respectively based on their electrical properties [54]. Table 4 shows the classification of the different chemical species as hard, soft and intermediate.

Table 4: Hard and soft acids and bases (Adapted from Ref. 54)

	Hard	Soft	Borderline
Acids	H^+, Na^+, K^+, Mg^{2+}, Ca^{2+}, Co^{3+}, Cr^{3+}, Fe^{3+}	Cu^+, Ag^+, Hg^+, Cd^{2+}, Pt^{2+}, Te^{4+}	Fe^{2+}, Co^{2+}, Zn^{2+}, Cu^{2+}, SO_2
Bases	H_2O, OH^-, F^-, Cl^-, $RCOO^-$,NH_3	R_2S, R^-, I^-, $S_2O_3^{2-}$, C_6H_6	SO_2^{2-}, NO_3^-, Br^-, pyridine, imidazoles

1.5.3 Advantages of MOFs as Membrane Materials

- *Easy to synthesize* – Due to coordination bonds being present in MOFs, lower activation energies are required for their fabrication and so even room temperature syntheses have been reported. In comparison, zeolites require harsher conditions like very high-temperatures and pressures
- *Fewer post-synthetic steps* – Most of the MOFs are grown in smaller solvents, unlike zeolites that have large solvent molecules trapped in their cages. Thus MOFs do not need high temperature activation or ion exchange, etc. to activate the structures by removing these solvent molecules
- *Metal centers capable of host-guest interactions* – Typically, metal sites in MOFs are capable of interacting with the guest molecules, leading to preferential adsorption and thus better performance
- "Gate-opening or breathing effect" – Because of host-guest interactions and ligand flipping (in ZIFs), most of the MOFs show flexible pore sizes. This

breathing effect makes them interesting, both from a chemistry standpoint, and for growing them as **membranes for gas separations**

In this section, we have seen that application of membranes for gas separations leads to significant energy reductions and that MOFs are uniquely suited for several industrially important gas separations because of their surface chemistry. In the following section, the story is further developed by talking about

- Different ways of providing energy for conducting MOF reactions,
- Synthesis techniques for MOF thin films and membranes, and
- Advantages of using microwaves for MOF membrane synthesis

CHAPTER II

BACKGROUND

2.1 Supplying Energy Required for MOF Synthesis

Omar Yaghi coined the term “Metal-Organic Framework” in 1995 for an interesting material his group had prepared [55]. MOF’s can be synthesized both at room temperature as well as at elevated temperatures. For synthesis at higher temperatures, different techniques are used for supplying energy.

2.1.1 Conventional Heating

Conventional heating refers to reactions carried out by energy input from electrical heating (includes normal convection ovens, furnaces, etc.). Two main classifications exist in conventional synthesis – solvothermal and non-solvothermal [56]. Solvothermal reactions are defined as reactions taking place in closed vessels at greater than saturation pressure, meaning at temperatures above the boiling point of the solvents [57]. Consequently, non-solvothermal reactions are defined as reactions that take place at sub-boiling point temperatures. Initially, most of the MOF syntheses were carried out at room temperature [58], where the reactants are just mixed by stirring at room temperature and most of them have good stability.

2.1.2 Alternative Synthesis/Heating Techniques

Alternative synthesis routes using different energy sources are essential to unlock potentially useful new structures with different size distributions and

morphologies. This is important from the structure-property- performance- process tetrahedron in material chemistry shown in Fig 5.

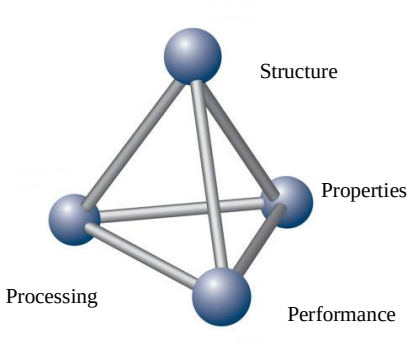

Fig 5: The traditional paradigm of materials

Different crystal sizes are needed for different MOF applications. For example, nanocrystals are necessary sometimes for developing the MOF's for catalytic, adsorption and separation applications while larger single crystals are necessary for determining the structure of the MOF. All these properties are dependent on duration and quantity of energy applied to the reactants, which in turn is determined by what is the energy source [59].

- *Microwave-assisted synthesis* - Microwave heating is very efficient since the radiation energy directly heats up the reaction mixture without any significant losses due to conduction and convection. It is not uncommon to observe significant enhancements in reaction rates due to homogenous heating of the mixture
- *Electrochemical synthesis* - First reported by researchers from BASF in 2005 [60], electrochemical synthesis of MOF's avoids the presence of problematic

counter anions like nitrates, etc. This is of importance to industry because of corrosion issues during process operation

- *Mechanochemical synthesis* - This synthesis involves inducing a chemical reaction by breaking intra-molecular bonds by mechanical forces. Mechanochemical synthesis is environment-friendly because organic solvents can be completely avoided [61]. Other added benefits include short reaction times, small particle sizes, better yields and harmless reaction by products like water
- *Sonochemical synthesis* - This involves the application of high energy sound waves to induce bond breakage, energy release and chemical reactions. It is a fast, simple, and environment-friendly method, which might help in the synthesis scale-up to industry

2.2 Synthesis Techniques for MOF Thin Films and Membranes

In general, MOF thin films and membranes are grown on substrates such as silica, alumina, titania, etc. for getting better mechanical stability. MOF membranes need to minimize the grain boundaries in order to reduce the non-selective inter-crystalline transport through these defects. Thus, they should be continuous, inter-grown and defect free to be useful as gas separation membranes. Long-term chemical and thermal stability is also important condition for MOF's to be successful as membrane materials.

2.2.1 Challenges with Fabrication

Fabricating MOFs into decent quality membranes is extremely challenging because heterogeneous nucleation (that is required for growing films and membranes on supports) is unfavourable. Another major obstacle is the fact that most of the organic linkers used for growing MOF's do not have additional functional groups capable of forming strong bonds with the hydroxyl groups on the surface of porous substrates. This causes poor interaction between the films and substrate surface leading to lack of mechanical stability of membranes. Even though zeolites require harsher conditions and bigger solvents for their synthesis (Section 1.5.3), the structures are more stable and the synthesis is more robust [62]. In general, the main issues associated with MOF membranes are as follows:

- *Poor membrane-substrate interaction* - As a general indicator, any MOF film/membrane which still retains most of its crystals (~70-80%) even after extended sonication (at least 1 hour) can be called having strongly attached to the support surface [63]. Some techniques reported for improving the attachment of films on the porous substrate surface are
    - Improving secondary bonding (hydrogen bonding and van der Waals interaction) by use of polymer binders [46], [64] and graphite coatings [65]
    - Providing covalent attachment by modification of the support surface with suitable chemistry [50], [66]
    - For example, Caro and co-workers were able to fabricate continuous well inter-grown ZIF-90 membranes by using 3-aminopropyltriethoxysilane (APTES) as a covalent linker forming a

bridge between the alumina substrate and the ZIF-90 crystals (Fig 7) [67]. This was possible because the ethoxy groups in APTES first formed strong bonds with the hydroxyl groups on the substrate surface. The amine groups on the other end of APTES reacted with the free aldehyde groups in the ligand (ICA) via imine condensation. On the contrary, without APTES, no continuous membrane could be obtained

- *Poor membrane stability* - Most MOFs are instable in contact with ambient conditions like humidity, etc. due to the reactions of either carboxylates or hydroxyl groups with moisture. There are a couple of reports about the improvement of IRMOF-3's resistance to moisture. In one of the publications, framework structure was imparted hydrophobicity by introducing long alkyl chains [68]. The other one reported coating the surface of IRMOF-3 membranes with a surfactant to make the membranes resistant to moisture [69]
- *Crack formation during activation* - Cracks form in polycrystalline MOF membranes when the membranes are cooled down following synthesis. Several of the MOF's like HKUST-1 [66], ZIF-69 [48], etc. have been shown to require slow cooling. The probable reason for crack formation during this cooling process is that porous supports cool down more rapidly than the MOF films leading to mechanical stresses. Even drying of MOF films can lead to crack formation because of surface tension effects at the interface in MOF films. Slowing down of the drying rate helps to reduce this effect

2.2.2 Different Strategies for Synthesis of MOF Thin Films and Membranes

There are several different strategies for growing MOF thin films and membranes however they can be broadly classified into the following

- *Direct growth* - Supports are immersed in the metal and ligand precursor solutions. Energy input by either conventional means or by alternate techniques leads to nucleation, from which crystals and finally inter-grown films and membranes (thickness of several μm's) can be obtained. However, some chemical modification of the supports is necessary to achieve heterogeneous nucleation on the support surface
- *Layer-by-layer (LbL) growth* - The substrate is first functionalized with SAMs (self-assembled monolayers) and then immersed in the precursor solutions for several cycles. During each step, it is possible to precisely control the thickness, orientation and homogeneity of the MOF films formed each time. The LBL technique is very effective for the synthesis of MOF films
- *Seeding and secondary growth* – This offers better control over MOF microstructure as compared to direct growth. However, it involves the additional step of coating the support surface with seeds. Thus, the quality of films and membranes obtained by secondary growth depend on how strongly the seed crystals are attached to the substrate surface
- *Chemical solution deposition* – It is a simple, rapid and very effective technique for growing MOF thin films. In this, substrates are spin or dip coated with nanocrystals from their dispersions. Multiple coatings can be performed if films of greater thickness are necessary

2.2.3 Synthesis of MOF Thin Films

There are subtle differences between the synthesis of MOF thin films and membranes. Hence they are discussed separately. A number of deposition methods are in use currently to produce continuous MOF films. A brief discussion about some of them is provided below

- *Direct solvothermal growth* - The substrate is immersed in a dispersion of MOF nanocrystals. However, to obtain a uniform coating of those crystals, the substrate needs to be functionalized or chemically modified with termination groups that are capable of forming bonds with the MOFs. This is frequently done by using self-assembled monolayers (SAM)s, which are ultrathin organic films that can very easily be coated onto the substrate
- *Direct-oriented solvothermal growth* - This is very similar to the above strategy except that now depending on the termination group of the SAM, crystals with different orientations are obtained [70], [71].
- *Microwave-induced thermal deposition* – This involves coating the surface of substrates with a thin layer of electrically conductive material like graphite and introducing MW irradiation when these substrates are immersed in the precursor solutions. High instantaneous temperatures are obtained near the support surface coated with graphite because of interaction with MW. This creates a sort of "reaction zone" on the surface, leading to growth of continuous MOF films. Yoo and Jeong reported continuous and homogeneous films of MOF-5 [63] by this method
- *Colloidal method* – Substrates are dip coated to obtain thin MOF films by immersion in colloidal gels of nanocrystals. This dip-coating can be repeated

multiple times depending on the thickness of the film required. However, the films are not strongly bound to the surface. Ferey et al demonstrated this method for the MOF MIL-89 [72]

- *Electrochemical synthesis* – Arbitrarily oriented films of MOF-5 (4-20 μm) have been deposited on the anode used for the electrochemical synthesis [73]. The growth is self-terminating and occurs only at electrically connected positions on the substrate

Some of the newer techniques for growing MOF films include evaporation-induced crystallization [74], gel-layer synthesis [75] and layer-by-layer technique [76].

2.2.4 Synthesis of MOF Membranes

The different synthesis techniques for growing polycrystalline MOF membranes can be broadly classified into two categories: in-situ growth and secondary growth [77]. In-situ growth is a very simple technique in which the modified/unmodified substrate is immersed in the precursor solutions. Nucleation and growth of crystals into films occurs in a single step, thus resulting in generally thicker membranes. Control of microstructure is also extremely difficult with this method. Secondary growth is a two-step process in which preformed MOF seed crystals are deposited on the substrate surface (by different methods), from which the membrane is formed by intergrowth. This technique has been shown to allow better control over microstructure, form thinner membranes and is somewhat independent of the type of substrates used for growing the membranes [78]. Different synthesis approaches that have been employed so far under both these categories are as follows

- *In-situ/direct growth on unmodified supports* - As the name suggests, this technique involves the in-situ synthesis of membranes from the mother precursor solutions in a single step. The synthesis does not involve any substrate modification. MOF-5 [50], ZIF-8 [45] and ZIF-69 [48] membranes have been successfully synthesized by this method previously. This was possible because of the favorable bond formation between ligand and hydroxyl groups on alumina surface. In general, heterogeneous nucleation on unmodified supports is unfavorable and membrane fabrication by this technique is difficult
- *In-situ/direct growth on modified supports* – Poor interaction between the MOF membrane and the unmodified substrate makes them unstable and not viable for their application as gas separation membranes. Chemical modifications of the substrate can improve the bonding and lead to continuous membranes. ZIF-8 [50] and ZIF-90 [67] membranes were grown by the surface modification techniques by Jeong et al and Caro et al respectively. Kwon et al developed an elegant in-situ solvothermal method using the counter-diffusion of precursor ions to grow membranes without any substrate modification as well [36]. Because of counter-diffusion, crystals grew from inside the support outwards, thus showing excellent mechanical stability
- *Seeded secondary growth* - This method involves first depositing a layer of preformed MOF crystals on the substrate surface, which then act as seeds from which the membranes are grown by solvothermal method. By controlling the seed layer properties like crystal size, its thickness and its

orientation, it becomes possible to control different aspects of MOF membrane microstructure like grain boundaries, thickness, etc. Further, since a seed layer is now present, secondary growth reduces the effect of the type of substrate used for membrane growth. It is essential to form seed crystals that are nano-sized for growing into membranes by secondary growth [79]. Several techniques are available for coating these seed crystals on to the substrate surface including manual rubbing [64], dip coating, spin coating, thermal deposition [64], using polymer binders [47], microwave-assisted seeding [81] and reactive seeding (when seeding is done in same step as in-situ growth) [80]. Some of the techniques for growing MOF thin films like MITD [63], LbL [76], etc. can be employed ingenuously for growing MOF membranes. This is because these films can serve as seed layers from which thicker, better inter-grown membranes can be obtained

- *Post-synthesis modification* - Post-synthesis modification is often employed to improve the stability of MOFs, adjust the pore sizes and provide additional functionalities like hydrophobicity, increased gas uptake, etc.

2.3 Microwaves and Their Advantages

Microwaves are a very reliable and efficient source of heating. In this section, the readers are introduced to the fundamentals of microwave first, followed by the benefits from using microwaves. Finally, a small description of the development of microwave ovens and the challenges in choosing the right conditions are discussed.

2.3.1 Fundamentals of Microwaves

As shown in Fig 6, microwave is an electromagnetic radiation (consisting of alternating electric and magnetic fields) which falls in the longer wavelength end of the electromagnetic spectrum with frequencies of 0.3 to 30 GHz [82], [83].

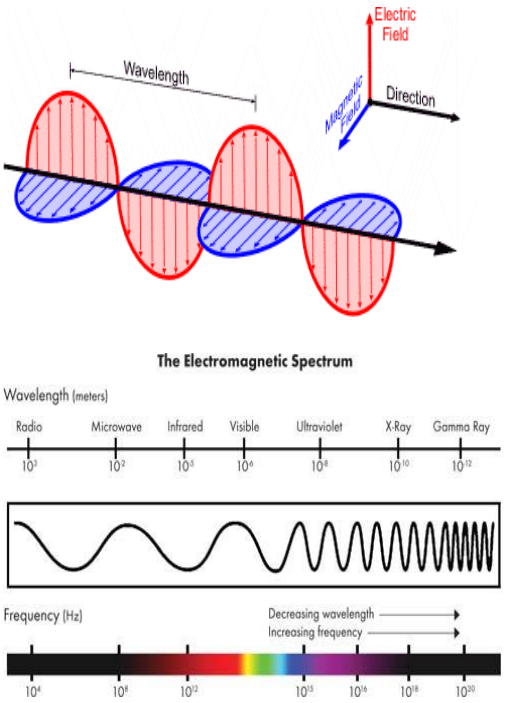

Fig 6: Components of microwave (above) and electromagnetic spectrum (below)

The two fundamental means by which energy is transferred to the reaction mixture from microwave irradiation are dipole rotation and ionic conduction [82].

In dipole rotation, the molecules with dipole moments try to align themselves with the external electric field due to the MW and do so by rotation. As these dipoles try to orient themselves by this rotation, energy transfer occurs. Thus highly polar solvents like water and methanol are best suited for use in MW-assisted synthesis.

Ionic conduction refers to the rapid increase in temperature due to microwave heating interacting with any free or conducting ions in the substance being heated.

2.3.2 Reaction Kinetics with Microwaves

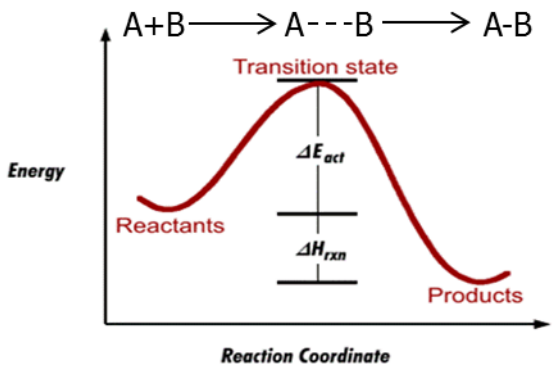

Fig 7: Typical reaction coordinates

According to the collision theory of reactions (Fig 7), there is activation energy (E_a) which needs to be overcome to form the products. MW helps the reaction to proceed quicker by enabling the reactants to overcome this activation energy barrier faster. Because of the speed at which energy transfer occurs with microwaves, very high instantaneous temperatures are achieved. Molecules now possess more energy to move about, collide and bring about the reaction. Thus, significant rate enhancements become possible as a result of

- Uniform heating
- Different transition states and reaction intermediates
- Superheating of solvents beyond their normal boiling points

- Creation of hot spots

The increase in temperature and corresponding rate enhancement are directly proportional to the intensity of microwave irradiation.

2.3.3 How Is Microwave Heating Different from Conventional Heating

Another reason for MW providing rapid heating is the way the energy is delivered. In conventional methods of heating, the heat is transferred to the reactant mixture through a conducting surface like the reaction vessel (glass or Teflon autoclave). This is slow and results in conduction energy losses. With MW heating, the heat is delivered directly to the reactant mixture by molecular interactions and thus it is very efficient and quick (Fig 8). In particular, when the reactor is transparent to microwaves, microwaves can only heat substances which are capable of interacting with it.

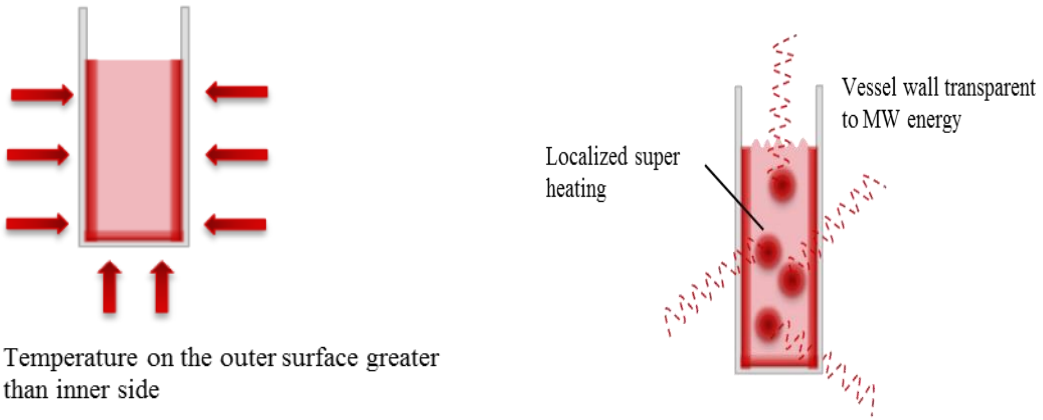

Fig 8: Heat transfer mechanisms of (left) conventional and (right) microwave heating

2.3.4 Advantages of MW-Assisted Synthesis

The main reasons for using MW in MOF synthesis are as follows [83]

- *Shorter synthesis times* – Faster reactions because of rate enhancements
- *Crystal size reduction* – Smaller size crystals are usually obtained when the rate of nucleation is high. In the case of microwaves, due to localized high temperatures, nucleation rates are enhanced and high concentrations of nuclei are formed. As the crystals grow from these nuclei, the reactant gets consumed. This in combination with shorter synthesis times ensure that small crystals with homogenous size distribution is obtained
- *Phase-selective synthesis of certain MOF's* – Since microwaves typically lead to rapid crystallization, it is possible to kinetically trap the crystal structures in the useful but unstable intermediate phases. During conventional heating, due to slower nucleation and growth, the crystals always end up in the stable phases

2.3.5 Microwave Ovens and Reaction Conditions

Chemists first began using commercial microwave ovens during the 1980's. The method was very crude, with the reactants put in a sealed vessel, held down with sand for cooling and the MW oven on defrost or cook. Lot of explosions and accidents occurred because of this and there was also lot of variability and uncertainty associated with using different microwave models. With time and improvement in technology available, companies began making more standardized ovens. In specific, companies which made specialist MW instruments for the

pharmaceutical industry began developing table top devices for laboratories. Many of these devices allow for temperature and pressure control and include design features like blowing cold air periodically to prevent explosions from happening. Microwave conditions are very important for successful and safe synthesis but finding the optimized conditions is tricky and takes a lot of trial and error. However, once the right MW power and duration have been identified, the setup can be used to conduct tests almost continuously.

In the next section, the microwave-assisted seeding followed by secondary growth technique for growing ZIF-8 membranes developed in our group is discussed. Following this, the equations used for calculating membrane permeances are presented and finally, some of the characterizations performed are summarized very briefly.

CHAPTER III

SYNTHESIS TECHNIQUE, EQUATIONS AND CHARACTERIZATIONS

As mentioned before, ZIFs exhibit flexible pore sizes due to “gate-opening effect” which arises from the flapping vibrations of the ligand molecule [52], [53]. This in combination with excellent stability make ZIF’s very interesting for separations of light hydrocarbons. In particular, ZIF-8 consisting of zinc metal nodes with 2-methyl imidazole as bridging ligands shows potential for the industrially important separation of propylene/propane [84]. They exhibit sodalite (SOD) structures with large cavities (11.6 Å) and pore apertures of 3.4 Å [51] (Fig 9).

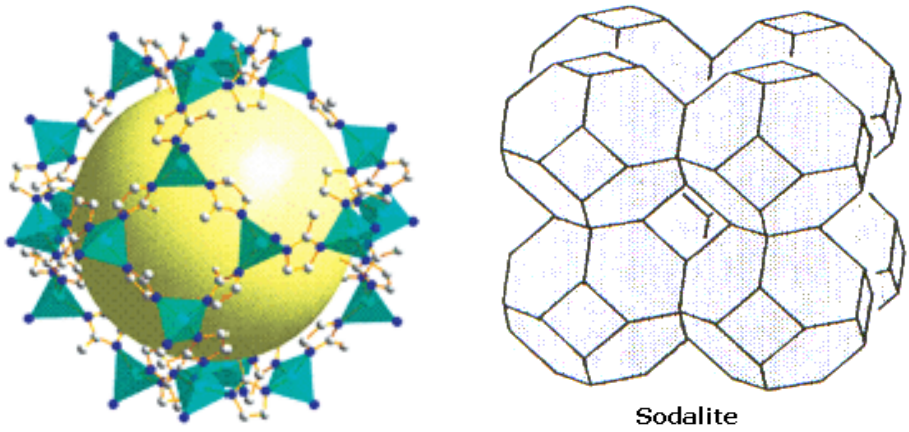

Fig 9: ZIF-8 (left) and Sodalite (SOD) (right) crystal structures

3.1 MW-Assisted Seeding and Secondary Growth

Several different synthesis protocols exist for growing MOF and ZIF films and membranes as mentioned before. Whatever the synthesis method, it is necessary to ensure heterogeneous nucleation on the surface of supports occurs in order to form

well inter-grown membranes. In-situ method is generally simpler and easier but it is very difficult to obtain the desired microstructures for the membranes. For this reason, though secondary growth is more complicated, it is the preferred synthesis technique to obtain membranes with good performance and tunable surface morphologies.

In the secondary growth method, seed crystals are anchored onto the porous supports like alumina, silica, etc., from which inter-grown films and membranes are obtained by secondary growth. As can be expected, the quality of membranes obtained is strongly dependent on how strongly the seed crystals are attached to the supports. The current seeding techniques like dip-coating, slip-coating and spin-coating are unable to ensure uniformity in seed crystal distribution and strong attachment of seed crystals.

This is where the significance of the seeding technique developed in 2013 by Kwon and Jeong comes into play. Densely packed ZIF-8 seed crystals are formed predominantly on the surface of porous α-alumina supports under microwave irradiation in a couple of minutes [81]. This concept is illustrated in Fig 10. These were then grown into ZIF-8 membranes by secondary growth by an aqueous recipe. In short, the alumina disc supports were first saturated with metal salts, following which they were immersed in ligand solution and subject to MW irradiation for 1.5 minutes. Since the support surface (“reaction zone”) has a high concentration of ions, these interact strongly with the MW energy, leading to increases in temperature and enhancement in reaction rates. This leads to greater heterogeneous nucleation and

smaller size crystals formed in a densely packed seed layer. The presence of phase-pure ZIF-8 seeds is shown by SEM images and XRD patterns.

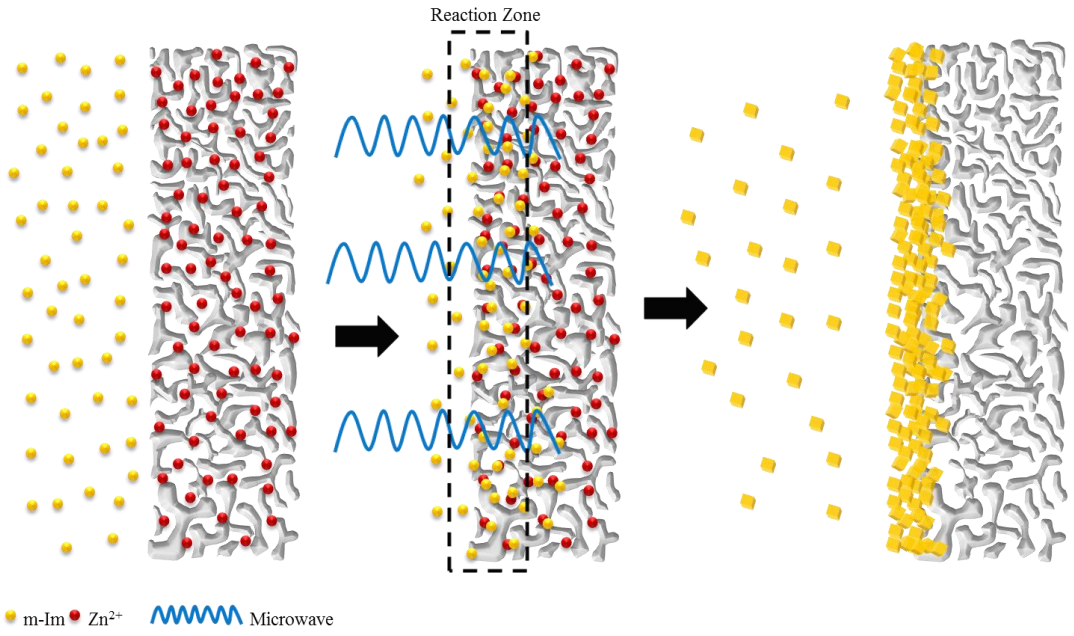

Fig 10: Schematic for the MW-assisted seeding technique developed (Adapted from Ref 81)

This method is fundamentally different from the MITD in that no conductive coatings are required and that heating occurs primarily due to ionic interactions with MW rather than through conduction through the graphite coatings. Thus, the seed layers grown by this technique retain ~ 80% of the crystals even after sonication for 2 hours. This could be possibly due to the covalent bonds formed between the surface hydroxyl groups of the support and the nitrogen in the ligands due to microwaves [50].

Subsequently the seed layers were grown into ZIF-8 membranes by a solvothermal aqueous recipe [85] and the optimum growth time was identified as 6 hours. Membranes synthesized by this technique were better than the other ZIF-8 membranes in the literature at the time with propylene permeances of ~ 200 (X 10^{-10} mol Pa^{-1} m^{-2} s^{-1}) and selectivities of ~ 40.

3.2 Gas Transport Through Membranes

According to Barrer [86], [87], gas transport through membranes involves a series of adsorption and diffusion steps. Each of these steps occurs as a result of an overall chemical potential gradient as the driving force and the kinetics of each step is determined by their activation energy barriers

- *Step 1* - Gas adsorption to membrane surface and then subsequent surface diffusion to the pore entrances
- *Step 2* – Adsorbed molecules enter the pores and settle down in the first energy minimum site available
- *Step 3* – Pore diffusion by hopping from one energy minimum site to the next and getting adsorbed
- *Step 4* – Gas desorption from the last energy minimum site in the pores followed by exit to the permeate side membrane surface. This is the reverse of Step 2
- *Step 5* – Gas desorption from the membrane surface to gas phase

3.2.1 Certain Membrane Definitions

Steady-state diffusive flux (J) as defined by Fick's First Law of Diffusion is determined by

$$J = -D \frac{dc}{dz} \approx -D \frac{\Delta c}{l} \quad (1)$$

Where D is the gas diffusivity (m^2/s), c is the concentration of the gas concentration on the membrane external surface (mol/m^3) and l is the membrane thickness along the direction of flow (m). If the Henry's Law regime is considered a valid approximation for the gas adsorption on the membrane, we have

$$J = -D \frac{dc}{dz} \approx -D \frac{\Delta c}{l} = -DK \frac{\Delta p}{l} \quad (2)$$

Where K is the solubility constant and Δp is the pressure difference across the membrane. Permeability (P) which is an intrinsic property of the membrane material, is defined as

$$P = J \frac{l}{\Delta p} = DK \quad (3)$$

In honor of Barrer, the common unit for permeability is Barrer. 1 Barrer = 3.348×10^{-16} mol $m^{-1}Pa^{-1}s^{-1}$. From Equation 3, it is clear that the permeability of the material is a combination of both the diffusivity and solubility of the gas in the

membrane. This arises as a consequence of the mechanism of gas transport through membranes described previously.

The permeance (Q) of the gas through the membrane can be measured, and is determined by

$$Q = \frac{P}{l} \tag{4}$$

The ideal selectivity of the membrane for a two-component gas feed (A and B) is a ratio of the pure single gas permeabilities

$$\alpha_{AB} = \frac{P_A}{P_B} = \frac{D_A}{D_B}\frac{K_A}{K_B} \tag{5}$$

The membrane separation factor for the same binary gas feed is defined as

$$\alpha_{AB} = \frac{\left({}^{y_A}/_{y_B}\right)}{\left({}^{x_A}/_{x_B}\right)} \tag{6}$$

Where y and x are the mole fractions of the gas components in the permeate and feed side respectively.

3.3 Characterization

Crystallinity and phases of the seed layers and membranes synthesized during this thesis were identified by a Rigaku Miniflex II X-ray diffractometer that uses Cu-Kα radiation with a wavelength of λ = 1.5406 Å. Scanning electron micrographs of

the top and cross-sections of the membranes were obtained from a JEOL JSM-7500F at an accelerating voltage of 5 keV. The gas separation performance of ZIF-8 membranes was tested at atmospheric conditions of temperature and pressure using a typical Wicke-Kallenbach setup (Fig 11). 50:50 mixtures of propylene and propane (total flow of 100 ml/min) were used as the binary gas streams at the feed side while the gas from the permeate side was collected and swept to the GC by argon with a sweeping flow of 100 ml/min. The composition of this swept gas was analysed using an Agilent Gas Chromatograph 7890A fitted with a PLOT Q column to identify propylene and propane peaks. Argon was used as the sweeping gas since it will not lead to any peaks on the gas chromatograph obtained using this specific column.

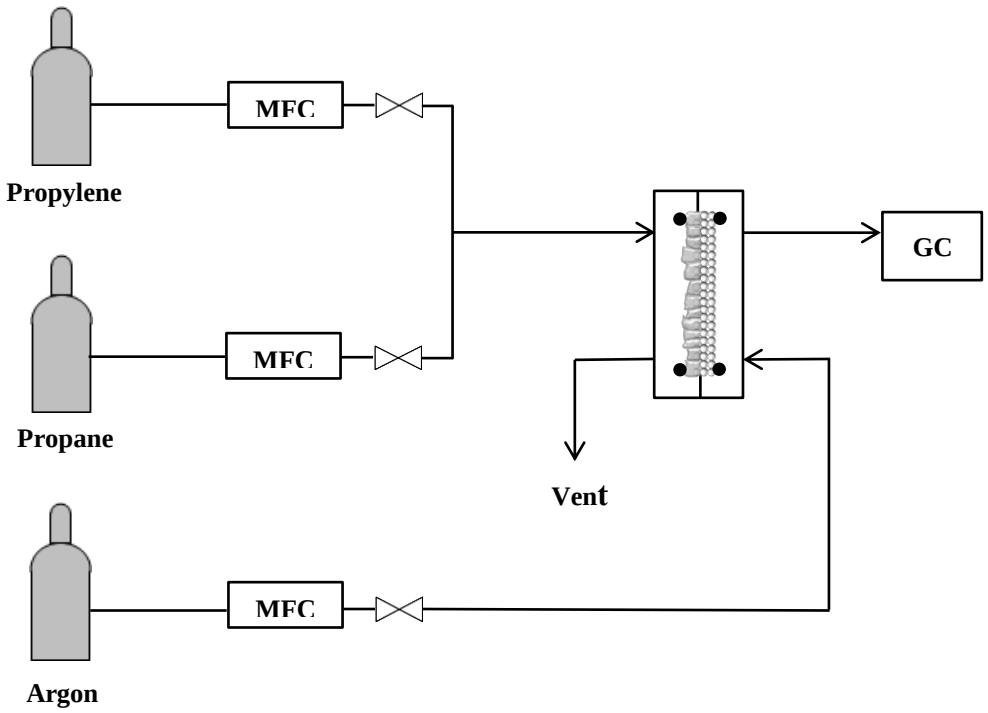

Fig 11: Wicke-Kallenbach setup used for binary gas performance measurements for the ZIF-8 membranes synthesized

CHAPTER IV

EFFECT OF DIFFERENT ZINC SALTS ON MORPHOLOGY AND PERFORMANCE OF ZIF-8 SEED LAYERS AND MEMBRANES

4.1 Introduction

As has been established previously, ZIFs are a subclass of MOFs, which show great promise for the separation of light hydrocarbons. In particular, ZIF-8 consisting of zinc metal nodes with 2-methyl imidazole as bridging ligands can be used in the industrially important propylene/propane separations because of their aperture size of 3.4 Å [84], [51].

Between the in-situ and secondary growth techniques for growing ZIF-8 membranes, secondary growth allows for greater control over membrane microstructure like thickness and grain boundaries. However the additional step of coating a strongly anchored seed layer on the support surface is essential before well inter-grown membranes can be obtained by secondary growth. Strong attachment of seed crystals to the substrate is difficult because of unfavorable heterogeneous nucleation and current techniques like spin and dip coating, etc. cannot achieve this effectively. In this regard, the MW-assisted seeding technique developed by Kwon and Jeong discussed in the previous chapter is useful for getting densely packed well attached layer of ZIF-8 seeds on alumina supports, which can then be grown into well inter-grown membranes by secondary growth in aqueous solution [81]. However, their synthesis used zinc nitrate as the zinc salt source for both seeding and secondary growth. While the membranes synthesized using zinc nitrate showed excellent permeance (208 mol $Pa^{-1}m^{-2}s^{-1}$) and selectivity (~40), they and no one else

have studied the effect of using different zinc salts as the metal source. It is expected that the rates of nucleation and solvation will be different for different zinc salts, leading to different morphologies of the seed layers and consequently different performance characteristics for the ZIF-8 membranes.

This arises due to a combination of Pearson's Hard-Acid Hard-Base theory and the Hoffmeister anion effect. As mentioned before, Pearson classified common elements into acids and bases of different strengths. Acids and bases of the same characteristics form salts with stronger bonds and thus their rates of nucleation will be lower. According to the Hoffmeister anion effect, the strength of solvation for different zinc salts will be determined by the counter anion in the zinc salt. Anions with a stronger electronic interaction will make the solvation of the zinc salt more difficult, thus affecting the growth kinetics during the secondary growth step.

Here, we present the results from a systematic study of the effect of different zinc salts on the ZIF-8 seed layers and membranes. The difference in thickness, grain sizes, grain shapes and grain boundary structures were investigated by X-ray diffraction, scanning electron micrograph images and binary gas performance measurements using the Agilent 7890A GC.

4.2 Experimental Section

4.2.1 Chemicals

Chemicals were used as purchased without further treatments and purification. Zinc nitrate hexahydrate ($Zn(NO_3)_2.6H_2O$, 98%, Sigma-Aldrich,), Zinc chloride anhydrous ($ZnCl_2$, 99.95%, Alfa Aesar) and Zinc acetate dehydrate ($Zn(CH_3COO)_2.2H_2O$, 97+%, Alfa Aesar) were used as metal sources. 2-

methylimidazole (m-Im) ($C_4H_5N_2$, 97%, Sigma-Aldrich) was the ligand. Sodium formate (SF) (HCOONa, 99%, Sigma-Aldrich) was the deprotonating agent to speed up the reaction. Methanol (99.8%, Alfa Aesar) was used as the solvent for seeding solutions and DI water was the solvent for the secondary growth.

4.2.2 Preparation of α-Al_2O_3 Disc Supports

First, polyvinyl acetate 500 (PVA, Duksan Korea) solution was prepared by dissolving 3g of PVA in 95 ml of DI water and 5 ml of 1M nitric acid (HNO_3). The mixture was stirred into a homogenous solution by heating and stirring at ~ 85°C for 1.5 hours after covering the beaker with aluminum foil. Once the solution cooled down naturally, it can be used for making alumina supports. The PVA plays the role of binder when the alumina powder is aggregated under high loads in a press. Then 10g of CR6 alumina powder from Baikalox, USA was added and ground with a pestle to remove big aggregates. To this, 1 ml of the prepared PVA was added and then this mixture was ground vigorously until a fine powder was obtained. Then 2.1g of this was pressurized in a mold at 10 tons of pressure for 1 hour. The obtained disc supports were then sintered in a furnace at 1100°C for 2 hours with ramping rates of 5°C for heating and cooling. The front side of the discs were then polished using a rotating polishing machine at 100 rpm using sand paper with roughness #1500. Good polishing is indicated when scratches are not visible on the surface under light. The polished discs are then sonicated in methanol for 1 minute to remove any flakes and then they are dried in a convection oven at 120°C for 1 hour before they are ready.

4.2.3 Formation of ZIF-8 Seed Layer

The metal precursor solution was prepared by dissolving 8 mmol of the different zinc salts in 40 ml of methanol while the ligand precursor solution had 31.5 mmol of m-Im and 1.8 mmol of SF in 30 ml of methanol. The polished, sonicated and dried alumina supports were placed vertically (with polished face slightly downwards) in a Teflon holder and then soaked in the metal precursor solution for 1 hour. After this, the metal-saturated supports were immersed in the ligand precursor in a microwave-transparent glass tube and immediately subjected to microwave radiation (100W and 1.5 minutes, CEM Microwave). Following cooling down to room temperature for 30 minutes, the seeded supports were washed in methanol under constant stirring for 24 hours to remove the excess precursor solutions from inside the supports by solvent exchange. The seed layers were then dried in a convection oven at 60°C for 4 hours to remove the methanol.

4.2.4 Formation of ZIF-8 Membranes

ZIF-8 membranes were obtained from these seed layers by secondary growth with DI water as the solvent [85]. Again metal and ligand precursor solutions were prepared separately by dissolving 0.37 mmol of the zinc salt and 27.6 mmol of m-Im, in 20 ml of DI water respectively. The metal solutions were then poured into the ligand precursor solutions to obtain homogenous mixtures under stirring. The seeded supports were then placed vertically in a Teflon holder in these solutions and subjected to secondary growth in an oven at 30°C for 6 hours. The membranes were solvent exchanged in fresh methanol under constant stirring but with a small change in washing time. The membranes were now washed with methanol only for 24 hours

as opposed to 5 days of washing according to the reported recipe. Finally the membranes were dried in a convection oven at 60°C for 6 hours to remove the methanol.

4.2.5 Characterizations

The crystalline phases for the different zinc salt ZIF-8 seed layers and membranes were tested by X-ray diffraction using the Rigaku diffractometer mentioned in section 3.3. SEM images for both the seed layers and membranes were taken in order to observe the morphology and thickness using the JEOL instrument with the specifications in section 3.3. The gas separation performance of the ZIF-8 membranes for a 50:50 mixture of propylene/propane was tested using a Wicke-Kallenbach setup and Agilent gas chromatograph with the conditions and setup illustrated in section 3.3.

4.3 Results and Discussion

For the case of synthesis using zinc nitrate as the metal source, densely packed ZIF-8 seed crystals are formed predominantly on the surface under microwave irradiation. This concept was illustrated in Fig 10.

As mentioned before, the number, size and location of the seed crystals depend strongly on the rates of nucleation and solvation for the metal ions. Rate of nucleation depends on the strength of interaction between the metal ion and counter anion in the metal salt, which is determined from the Pearson's acid-base theory. Strength of solvation is determined by the Hofmeister anion effect, which takes into account the surface charge density and the enthalpy of solvation for the counter

anions. It has been hypothesized from the Pearson's theory that the following rates of nucleation is observed for different zinc salts in [88]

$$Zn(NO_3)_2 > ZnCl_2 > Zn(CH_3COO)_2$$

Based on the Hofmeister anion effect, the following order for strength of solvation has been empirically estimated in [89]

$$Zn(CH_3COO)_2 > ZnCl_2 > Zn(NO_3)_2$$

Higher rate of nucleation means that rate of reaction is faster. This implies that more nuclei are going to be formed at the "reaction zone", from which a greater number of crystals are going to grow. However, since a large number of crystals are now growing, there is competition for the metal and ligand ions, and thus the crystals cannot grow to bigger sizes. Rather, this is going to result in a larger number of nano-sized crystals. For lower rates of nucleation, this competition is absent and thus the crystals are going to grow to bigger sizes.

Zinc salt sources having anions with weaker interactions with the solvent will have lower strengths of solvation and thus the solvated metal ions can more easily react with the deprotonated ligands, leading to faster crystal growth. In the case of counter anions leading to stronger interaction effect with the solvent, it is likely that the rate of crystal growth will be slower.

4.3.1 Seed Layers from Different Individual Zinc Salts as Metal Sources

The X-ray diffraction patterns for the different seed layers are shown below (Fig 12). All of them indicate phase-pure nano-sized ZIF-8 crystals which are

identified by the peak broadening as compared to the simulated pattern. Furthermore, as compared to zinc nitrate, zinc chloride and zinc acetate seed layers exhibit narrower peaks with larger intensities. Narrower peaks indicate larger crystals with short range order and greater crystallinity. This is further confirmed by the scanning electron micrographs of the seed layers (Fig 13).

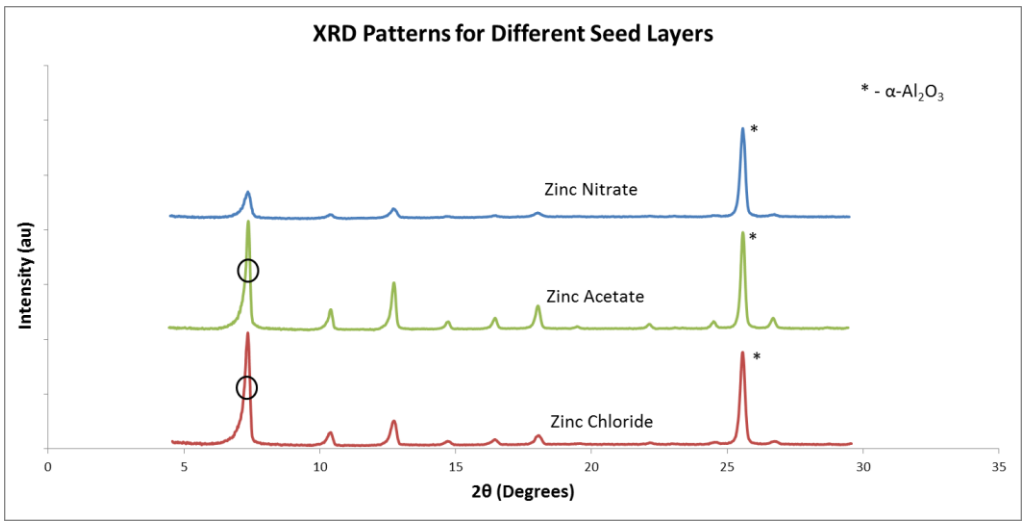

Fig 12: XRD for the 3 different seed layers (circles indicate narrower peak widths for zinc chloride and acetate)

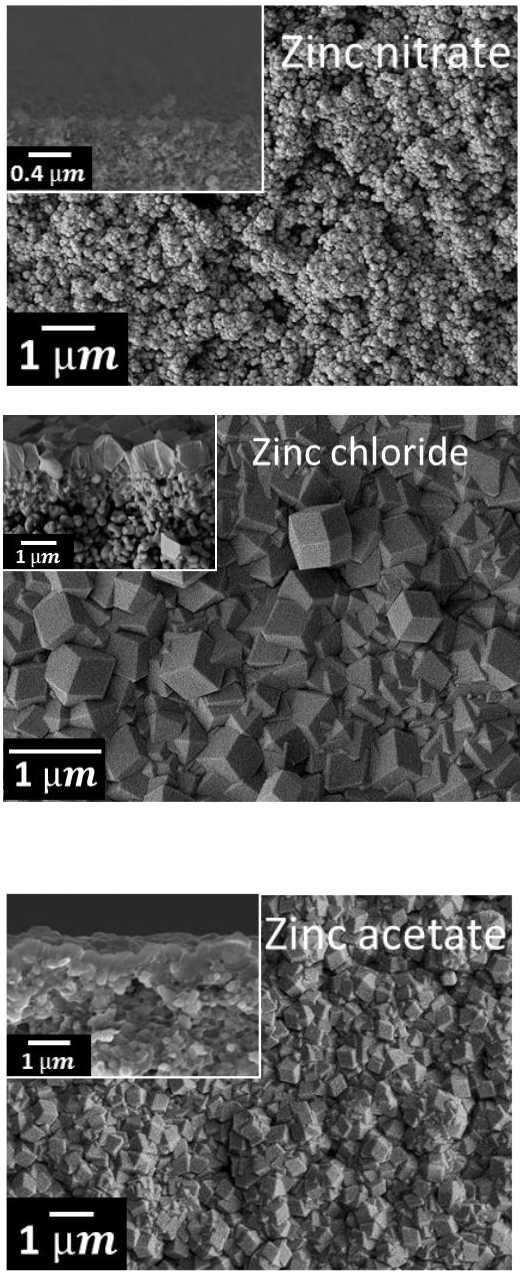

Fig 13: SEM images of top views and (inset) cross-sections for the different seed layers

As can be seen from the SEM images, the morphologies and crystal sizes are widely different for the seed layers from different zinc salts. Crystal sizes for zinc acetate and zinc chloride seed layers are much bigger and exhibit a size distribution.

However for zinc nitrate, densely packed seed layer consisting of uniform-sized small crystals is obtained. As explained previously, higher rate of nucleation leads to smaller crystals and lower rate of nucleation leads to bigger crystals. Since zinc nitrate has the highest nucleation rate among the 3 zinc salts, crystals in the seed layer are smaller and more numerous as compared to zinc chloride and zinc acetate.

These seed layers were then grown into ZIF-8 membranes by the secondary growth aqueous recipe using zinc nitrate for secondary growth (since the recipe followed used zinc nitrate for the secondary growth step). Following solvent exchange with methanol for 1 day and activation by drying for 6 hours, these membranes were tested for their binary gas separation performance using the W-K setup and GC. The results are presented in Table 5 while the X-ray diffraction patterns for these membranes are presented in Figure 14.

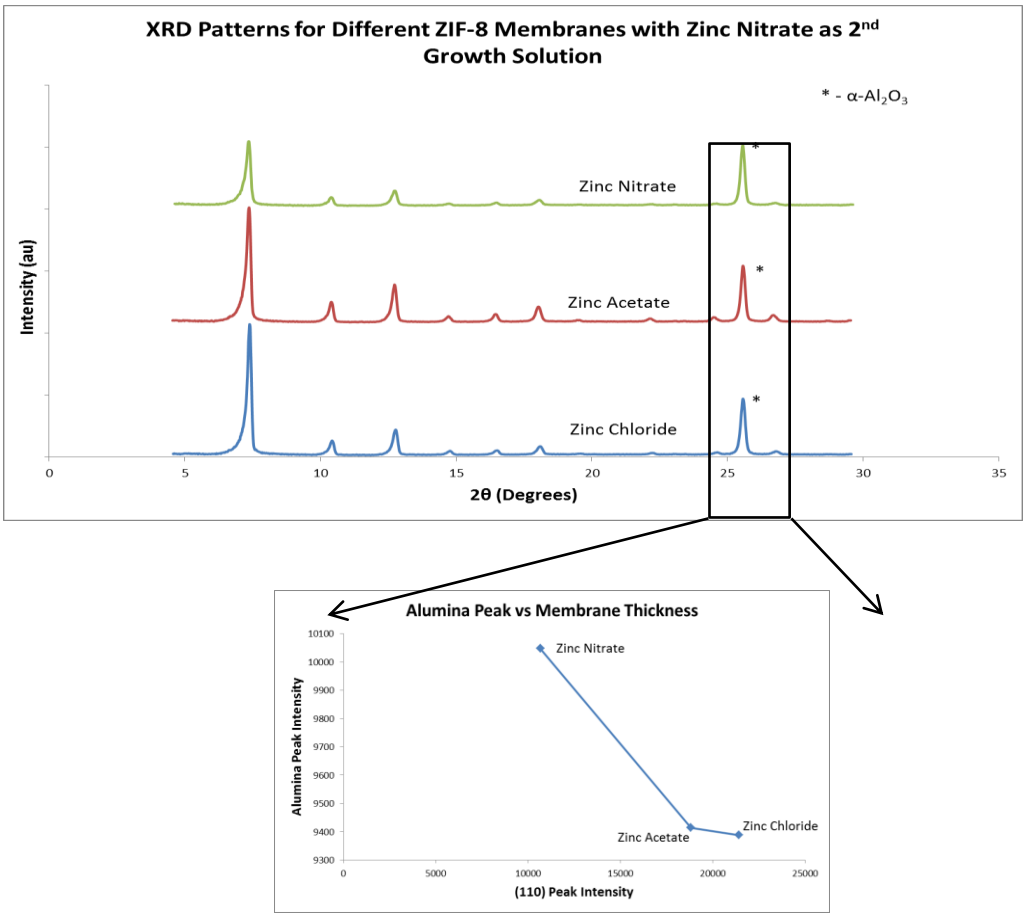

Fig 14: XRD for the 3 different membranes (reduction in alumina peak intensities is zoomed in)

Table 5: C_3H_6/C_3H_8 binary gas performance of ZIF-8 membranes from different zinc sources

Membrane Type	**Permeance (x 10^{-10} mol Pa^{-1} m^{-2} s^{-1})**		**Selectivity**
	Propylene (C_3H_6)	**Propane (C_3H_8)**	
Zinc nitrate	**268.29 ± 13.26**	2.61 ± 0.18	**104.49 ± 11.61**
Zinc chloride	**39.18**	N/A	N/A
Zinc acetate	**22.47**	N/A	N/A

The membranes from zinc chloride and zinc acetate seemed to indicate a very thick cross-section because of low permeance from the GC measurement, and higher intensities for the ZIF-8 peaks and reduction in alumina peak on the XRD patterns. It was decided to vary some reaction parameters like metal concentration and sodium formate concentration in the seeding precursor solutions to increase the rate of nucleation. It was expected that this would lead to formation of a greater number of seed crystals on the surface predominantly, making the seed layers similar to those from zinc nitrate (which showed good performance when secondary growth was performed). Metal concentration and sodium formate concentration were made twice as compared to the base recipe (M2X and SF2X respectively) keeping all other synthesis and activation conditions the same. Since it was not possible to dissolve the zinc acetate at these concentrations (solubility limit of zinc acetate was exceeded), only zinc chloride membranes were tested under these conditions and the results are presented in Table 6.

Table 6: C_3H_6/C_3H_8 binary gas performance of ZIF-8 membranes from zinc chloride seed layers with different synthesis recipe

Membrane Type	**M:L:SF Molar Ratios**	**Permeance (x 10^{-10} mol Pa^{-1} m^{-2} s^{-1})**		**Selectivity**
		Propylene (C_3H_6)	**Propane (C_3H_8)**	
M2_L1_SF1	1:2.33:1.48	**12.86 ± 1.11**	N/A	**N/A**
M1_L1_SF2	1:4.65:5.92	**18.83 ± 1.28**	N/A	**N/A**
M2_L1_SF2	1:2.33:2.96	**5.86**	2.38	**2**

The results from Tables 5 and 6 seemed to indicate it was possible to grow good quality membranes from zinc nitrate seed layers only and not from zinc chloride and zinc acetate. This can possibly be explained as follows:

- *Effect of nucleation rate on the seed layer morphology* – Higher nucleation rates (zinc nitrate) lead to numerous smaller size crystals. Densely-packed seed layers are thus obtained. When the nucleation rate is lower (zinc chloride and acetate), larger size crystals are formed and it is not possible to achieve as densely and close-packed layer as before. More crystals are formed inside the support as well, because of slower reaction rates
- *Effect of solvation and crystal growth rate during the secondary growth* – Zinc salts with counter anions having weaker solvent interaction effect (zinc nitrate) are likely to have greater crystal growth rate. This means that many crystals grow uniformly bigger and the average size of the crystals is almost same as the individual crystal sizes. Thus membranes possess better grain boundaries and show good separation performance. For zinc chloride and acetate seed layers (which are less densely packed), to achieve well inter-grown membranes with good grain boundary structure, the rate of crystal growth needs to be slower. Thus, it could be difficult growing zinc chloride and acetate seed layers to good quality ZIF-8 membranes using zinc nitrate as the metal source during secondary growth

Hence, it was of interest to investigate how the seed layer morphology and subsequent membrane performance would be affected by incorporation of zinc nitrate as a 50:50 mixture (by moles) with zinc chloride and zinc acetate in the seeding precursor solutions.

4.3.2 Seed Layers and Membranes from 50:50 Mixtures of Different Zinc Salts

The metal precursor solutions were prepared with the same total metal concentration as the reported recipe [83] but with 50:50 mixtures (by concentration) of zinc nitrate, with zinc chloride and zinc acetate respectively. All other synthesis parameters were kept the same as in the report [83]. The X-ray diffraction patterns again confirmed the presence of phase pure crystals of ZIF-8, with peak intensities approximately average of the values for the individual zinc salts (Fig 15). SEM images of the top and cross-sections for these 50:50 mixtures of seed layers indicated average properties of the two zinc salts used (Fig 16).

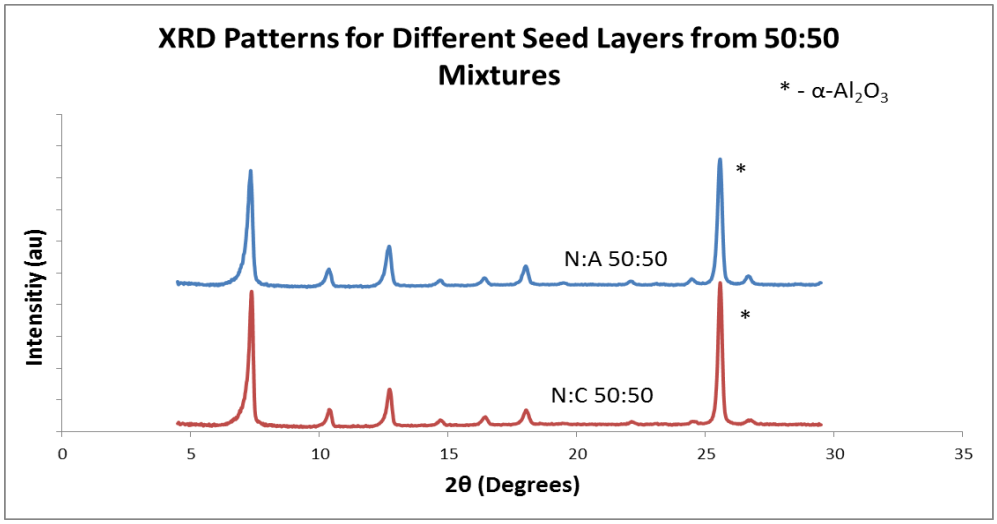

Fig 15: XRD for the different seed layers from 50:50 mixtures of zinc salts

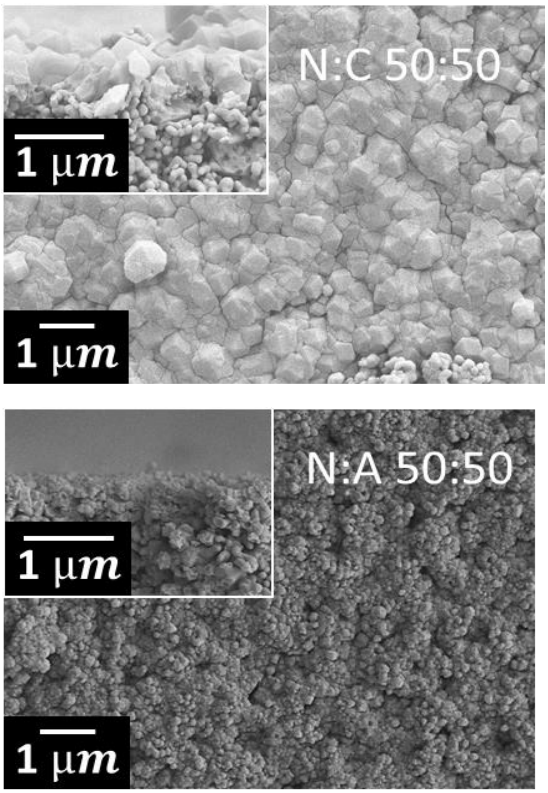

Fig 16: SEM images of top views and (inset) cross-sections for the different seed layers

These seed layers were then grown into membranes by using zinc nitrate as the metal source during the secondary growth step. The XRD (Fig 17) and binary gas separation performance (Table 7) again seemed to indicate membranes with thicker cross-sections but some of them showed good separation performance.

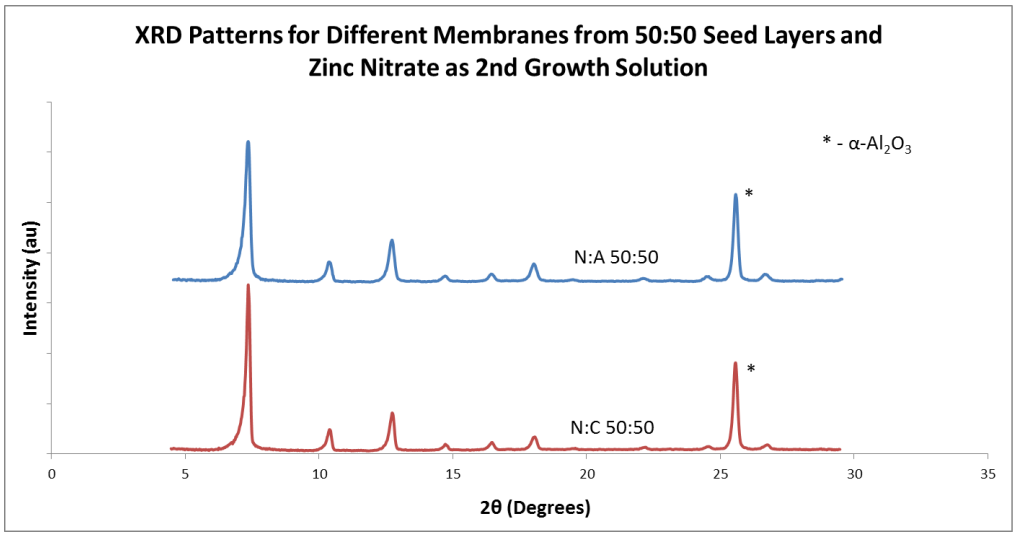

Fig 17: XRD for the different membranes from 50:50 seed layers

Table 7: C_3H_6/C_3H_8 binary gas performance of ZIF-8 membranes from 50:50 mixtures of different zinc sources

Membrane Type	**Permeance (x 10^{-10} mol Pa^{-1} m^{-2} s^{-1})**		**Selectivity**
	Propylene (C_3H_6)	**Propane (C_3H_8)**	
N:C	**18.08 ± 2.08**	1.74*	**12***
N:A	**41.26 ± 2.79**	1.2*	**38***

* - No standard deviation available since only 1out of 3 membranes showed propane permeance

The results shown in Table 7 seemed to indicate that probably zinc nitrate, with high nucleation rates leading to densely packed seed layers with small crystals, seemed to be most suited to this MW-assisted seeding followed by secondary growth.

As was hypothesized before, to grow good quality ZIF-8 membranes from zinc chloride and zinc acetate seed layers, rate of crystal growth during the secondary growth step should be slower. Thus, secondary growth for these seed layers was performed with the corresponding zinc salts as the metal sources instead of using the zinc nitrate based recipe. The metal concentration was maintained the same as for zinc nitrate based secondary growth recipe with all other synthesis and activation conditions the same as before. The X-ray diffraction patterns (Fig 18) for the membranes reveal that zinc chloride and acetate based membranes had larger size crystals with probably a thicker cross-section because of increased ZIF-8 peak intensities and reduction in the alumina peak intensity. The SEM images of the membranes corroborate the conclusions from the XRD (Fig 19). Binary gas separation performance (Table 8) for these membranes concluded that zinc chloride membranes do not show any separation performance while zinc acetate membranes have a higher selectivity but lower permeance as compared to zinc nitrate membranes. This again indicates a thicker cross-section. Figure 20 provides a comparison of propylene/propane separation performance of ZIF-8 membranes in this work with other membranes in literature. As can be seen, the membranes outperform most of the other membranes reported so far.

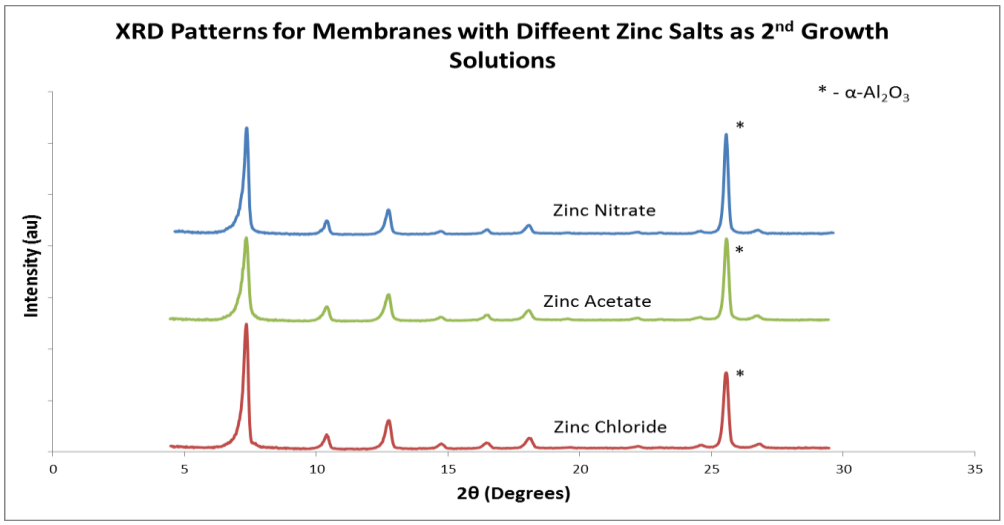

Fig 18: XRD for the different membranes from different seed layers and 2nd growth solution

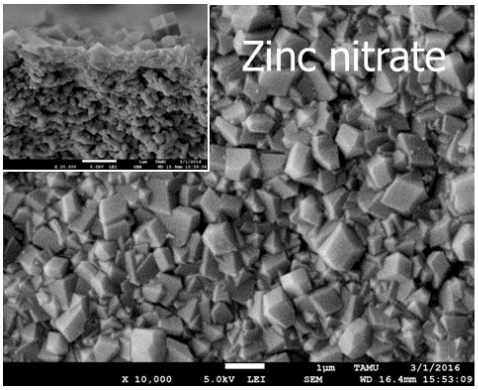

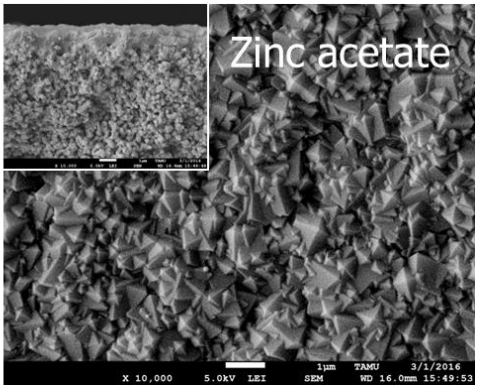

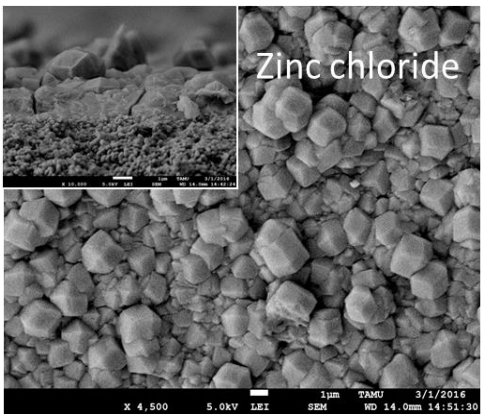

Fig 19: SEM images of top views and (inset) cross-sections for the ZIF-8 membranes from different 2nd growth solutions

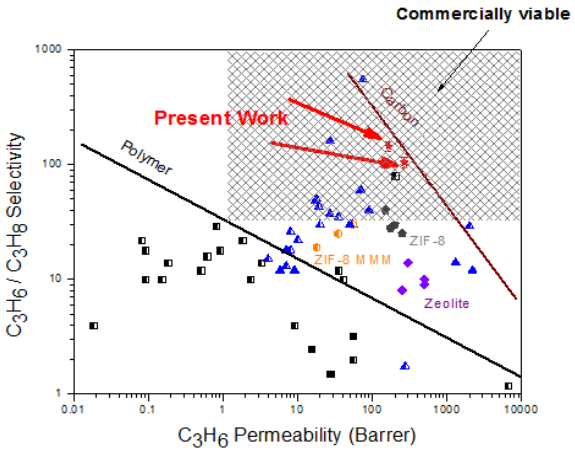

Fig 20: Comparison of propylene/propane separation performance with others in literature (Triangle: Carbon membranes, Square: polymer membranes, Diamond: zeolite membranes, Pentagon: ZIF-8 membranes, Hexagon: ZIF-8 mixed matrix membranes and Star: ZIF-8 membranes in this work)

Table 8: C_3H_6/C_3H_8 binary gas performance of ZIF-8 membranes from different zinc sources in the secondary growth solutions

Membrane Type	**Permeance (x 10^{-10} mol Pa^{-1} m^{-2} s^{-1})**		**Selectivity**
	Propylene (C_3H_6)	**Propane (C_3H_8)**	
Nitrate seed layer and Nitrate 2nd growth	**268.29 ± 13.26**	2.61 ± 0.18	**104.49 ± 11.61**
Chloride seed layer and Chloride 2nd growth	**2.95 ± 0.74**	1.19	**2.48**
Acetate seed layer and Acetate 2nd growth	**165.52 ± 14.58**	1.19 ± 0.21	**144 ± 12.73**

Based on these results, it becomes evident that different zinc salts play a crucial role in

- Seed layer morphology

- Intergrowth of these seed layers into good quality membranes

It was identified that ZIF-8 seed layers formed from zinc nitrate as the metal source seemed to exhibit most ideal microstructure (dense packing, uniformly small crystals) for secondary growth into membranes. Thus, the following section presents the results and discussion for the effect of using different zinc salts in the secondary growth solution for zinc nitrate-based ZIF-8 seed layers.

4.3.3 ZIF-8 Membranes with Different Zinc Salts in the Secondary Growth Solution

From the zinc nitrate based seed layers, ZIF-8 membranes were obtained by using different zinc salts as the metal source in the secondary growth solution. Concentrations for the different zinc salts was the same as for the zinc nitrate based reported recipe. The X-ray diffraction patterns (Fig 21) for the different membranes had similar peak intensities which possibly indicated that there are not significant differences in terms of membrane thickness. SEM images however highlight significant differences in grain boundaries, crystal sizes, shapes and inter-growth for the different membranes (Fig 22). Binary gas separation performance was also tested for the membranes using the Agilent GC (Table 9).

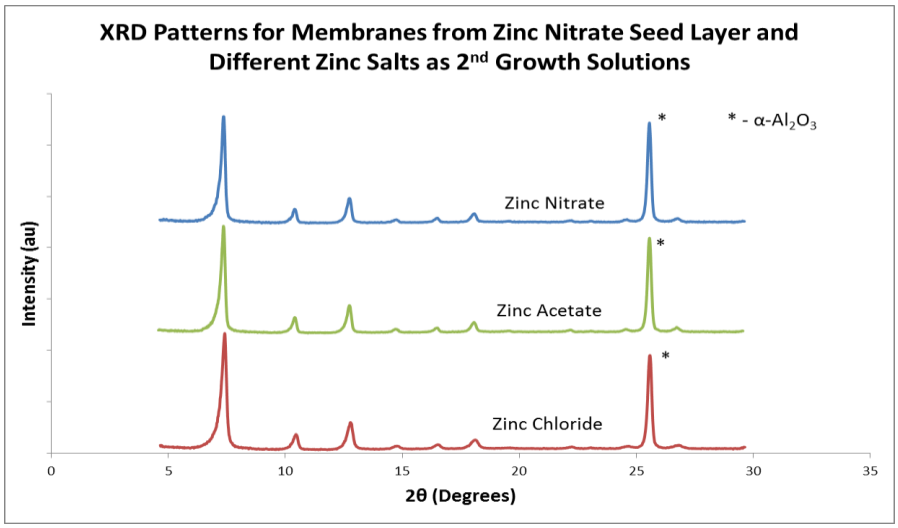

Fig 21: XRD for the different membranes from zinc nitrate seed layer and different 2nd growth solutions

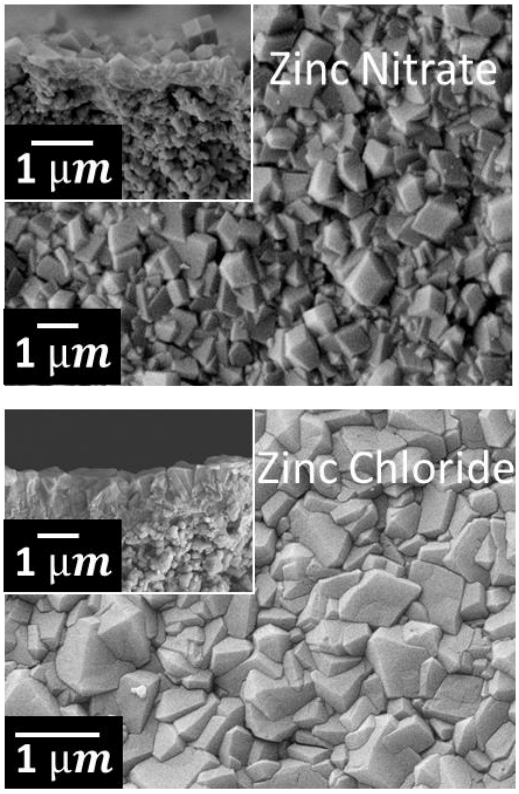

Fig 22: SEM images of top views and (inset) cross-sections for the ZIF-8 membranes from zinc nitrate seed layers with different 2nd growth solutions

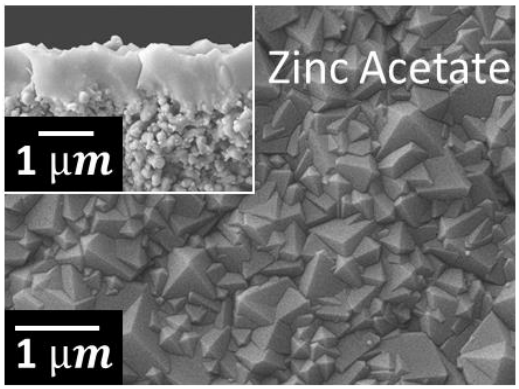

Fig 22 continued

Table 9: C_3H_6/C_3H_8 binary gas performance of ZIF-8 membranes with different zinc salts in the secondary growth solutions

Membrane Type	**Permeance (x 10^{-10} mol Pa^{-1} m^{-2} s^{-1})**		**Selectivity**
	Propylene (C_3H_6)	**Propane (C_3H_8)**	
Nitrate seed layer and Nitrate 2nd growth	**268.29 ± 13.26**	2.61 ± 0.18	**104.49 ± 11.61**
Nitrate seed layer and Chloride 2nd growth	**175.38 ± 46.79**	49.15 ± 32.33	**8.21 ± 5.12**
Nitrate seed layer and Acetate 2nd growth	**303.24 ± 6.06**	33.95 ± 8.12	**10.22 ± 2.26**

Though the overall microstructure of the membranes appears well inter-grown from the SEM images, they do exhibit significant differences. As discussed in section 4.3.2, zinc chloride and zinc acetate potentially lead to slower rates of crystal growth during secondary growth step. Thus, some crystals grow to bigger sizes leading to potentially poorer grain boundaries in comparison to zinc nitrate based

secondary grown membranes. These grain boundary defects (in the scale of nm) are difficult to observe under the resolutions offered by scanning electron micrographs. However, poorer grain boundaries lead to greater non-selective inter-crystalline transport of gases through the membranes. Thus, chloride and acetate secondary growth membranes had lower separation performance in comparison to nitrate membranes during the permeation measurements (Table 9).

To estimate the rate of crystal growth for different zinc sources in the secondary growth solutions, the change in surface morphology as a function of secondary growth time was captured by scanning electron micrograph images (Fig 23).

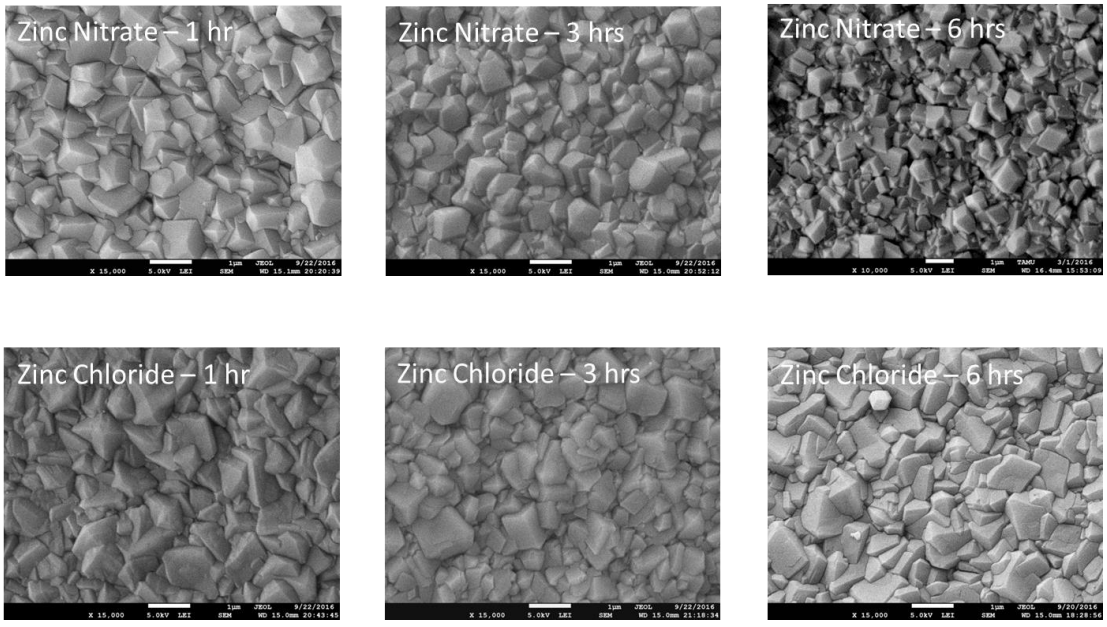

Fig 23: SEM images of the surface morphology for the ZIF-8 membranes as a function of time

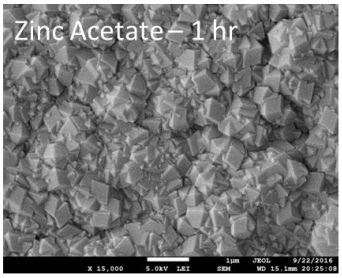

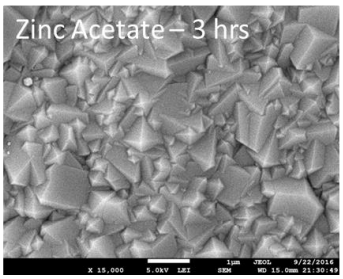

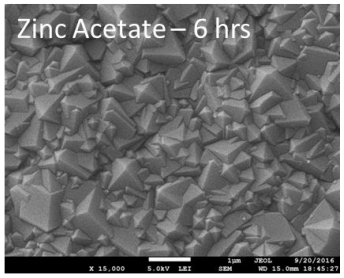

Fig 23 continued

From the SEM images, it can be clearly seen that each membrane has its own distinctive surface morphology and rate of growth for the crystals. For chloride and acetate membranes, it can be seen that preferential growth of bigger size crystals/grains is observed whereas for zinc nitrate membranes, all the crystals averagely grow to bigger sizes. A very crude estimate of the crystal sizes for each of the membranes yielded the following results (shown in Table 10 and Fig 24).

Table 10: Average crystal sizes and rough estimates of the rates of crystal growth

Membrane Type	**Average Crystal Sizes (nm)**			**Estimated Rate of Growth (nm/hr)**
	1 hour	**3 hours**	**6 hours**	
Nitrate seed layer and Nitrate 2nd growth	200	300	500	**60.53**
Nitrate seed layer and Chloride 2nd growth	400	500	600	**39.47**
Nitrate seed layer and Acetate 2nd growth	550	600	650	**19.74**

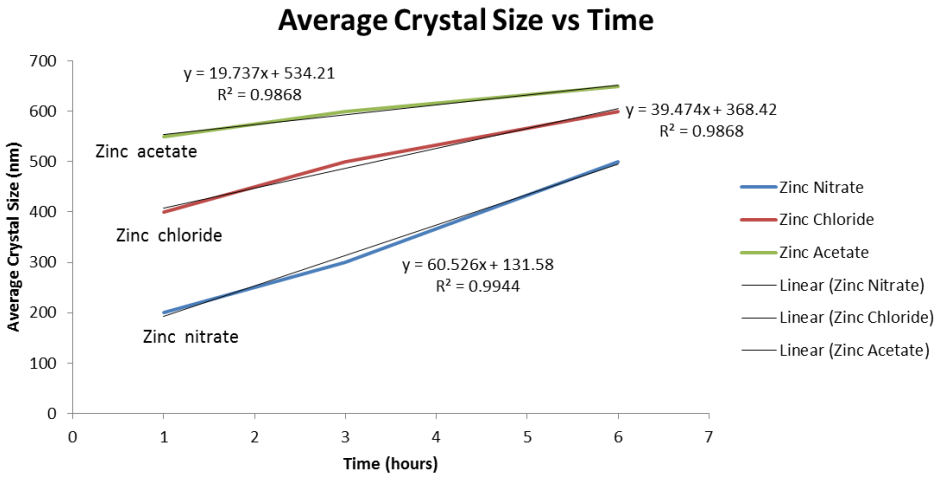

Fig 24: Plot of average crystal size vs time for the ZIF-8 membranes

The above estimates are approximate and qualitative in nature. The X-ray diffraction patterns for these membranes will provide a quantitative idea of the crystal growth rates when the peak intensities for ZIF-8 are plotted as a function of time. This data collection is currently in progress. It is however clear that due to difference in crystal growth rates, the size and shape of the crystals is different. It was hypothesized that crystals had slightly different shapes since crystal growth in different orientations/directions was different. This can be captured by plotting the relative peak intensities for the different peaks as a function of the first peak intensity. Different ratios would indicate different preferential growth and thus different crystal shapes for each zinc salt. The graphs representing this are presented in Fig 25. The error bars representing standard deviations are also shown here. The simulated XRD pattern for ZIF-8 (CIF database) with the peak indices indicated is shown below. The small difference in the intensity ratios does not indicate any significantly different preferred orientation for growth but can still be the potential

cause for the different crystal shapes with each zinc salt. SEM images of the powder samples for the different zinc salts will present more conclusive evidence and is also currently being taken.

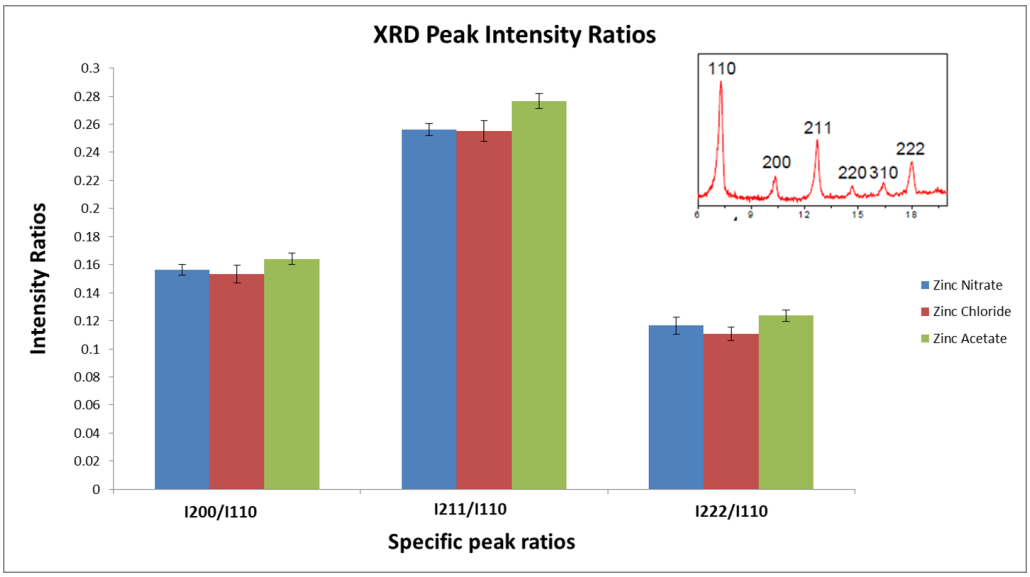

Fig 25: Plot of relative peak intensities for the different crystallographic planes

4.3.4 ZIF-8 Membranes with 50:50 Mixtures in the Secondary Growth Solution

To confirm that average properties are exhibited when different zinc salt combinations are used in the secondary growth solution with zinc nitrate seed layers, ZIF-8 membranes were synthesized using 50:50 mixtures (by moles) of different zinc salts. X-ray diffraction patterns (Fig 26), scanning electron micrographs (Fig 27) and binary gas performance (Table 11) of these membranes were collected.

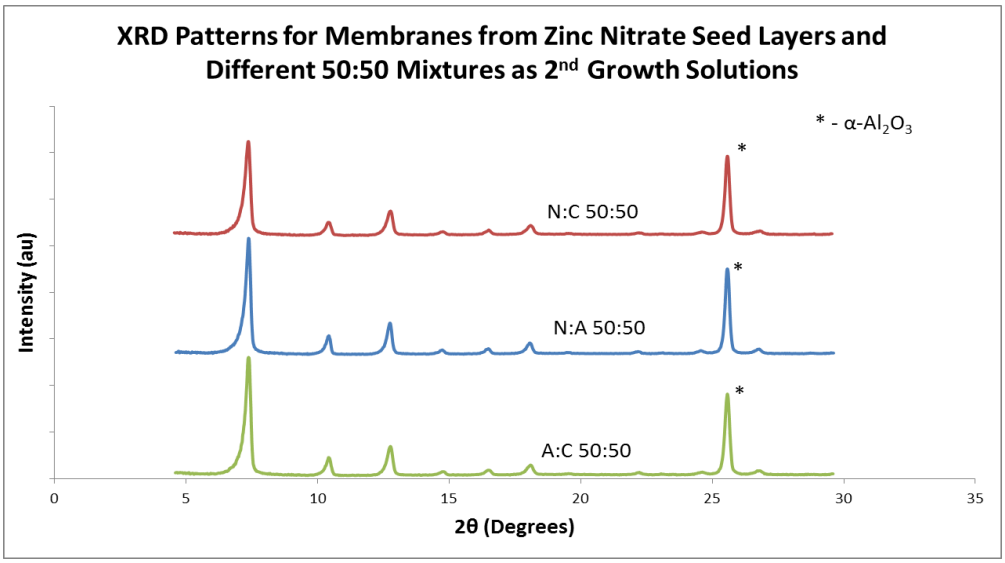

Fig 26: XRD for the membranes from zinc nitrate seed layer and different 50:50 mixtures of zinc salts as 2nd growth solutions

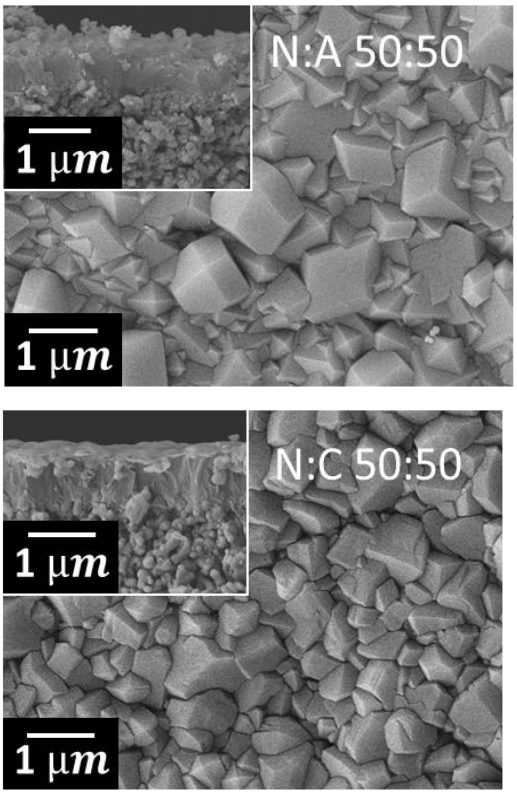

Fig 27: SEM images of the top view and (inset) cross-sections for the ZIF-8 membranes from zinc nitrate seed layers with 50:50 mixtures in 2nd growth solutions

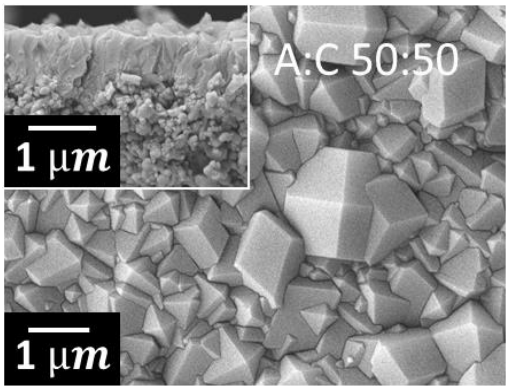

Fig 27 continued

The scanning electron micrographs clearly indicate average properties of the different zinc salts used, in terms of the membrane inter-growth and in terms of crystal sizes and shapes.

Table 11: C_3H_6/C_3H_8 binary gas performance of ZIF-8 membranes with 50:50 mixtures in the secondary growth solutions

Membrane Type	**Permeance (x 10^{-10} mol Pa^{-1} m^{-2} s^{-1})**		**Selectivity**
	Propylene (C_3H_6)	**Propane (C_3H_8)**	
Nitrate seed layer and N:A 50:50 2nd growth	**230.67 ± 6.91**	12.46 ± 6.12	**49.75 ± 11.65**
Nitrate seed layer and N:C 50:50 2nd growth	**205.81 ± 11.83**	32.81 ± 10.14	**10.68 ± 4.76**
Nitrate seed layer and A:C 50:50 2nd growth	**196.9 ± 4.86**	11.82 ± 3.88	**38.08 ± 10.91**

Though the introduction of zinc nitrate in the secondary growth solutions does improve the performance of the membranes, the selectivity values still indicate the presence of potentially poor grain boundaries. It is interesting to note that A:C membranes exhibit lower permeances but higher selectivities in comparison to N:C membranes.

4.4 Conclusions

In conclusion, we performed a systematic study on the effect of different zinc salts on the seed layer morphology and consequently membrane performance. ZIF-8 seed layers and membranes synthesized from different zinc salts had different morphologies and performances due to different rates of nucleation and crystal growth for each zinc salt. For the MW-assisted seeding technique followed by secondary growth, it was determined that zinc nitrate seed layers (densely packed with uniform small crystals) had the best morphology for membrane growth in the aqueous secondary growth step. This was potentially due to ability to form membranes with excellent grain boundaries following secondary growth. However, we were also able to synthesize high quality ZIF-8 membranes from zinc acetate seed layers using zinc acetate as the metal source in the secondary growth step. As a result, the effect of different zinc salts, with different crystal growth rates, on the secondary growth step was subsequently investigated. It was concluded that, for zinc nitrate seed layers, rate of crystal growth should ideally be higher to form membranes showing good performances (permeances ~ 200 mol Pa^{-1} m^{-2} s^{-1} and selectivity ~ 100). When 50:50 mixtures (by concentration) of different zinc salts were used in

both the seed layers and secondary growth step, average properties for seed layer morphology, membrane thickness and grain boundaries were observed.

CHAPTER V

MW-ASSISTED ONE-POT SYNTHESIS OF ZEOLITIC IMIDAZOLATE FRAMEWORK (ZIF-8) FILMS

5.1 Introduction

In the previous chapter, we saw that ZIF-8, consisting of zinc metal nodes with 2-methyl imidazole as bridging ligands can be used in the industrially important propylene/propane separations because of their aperture size of 3.4 Å [84], [51]. The secondary growth synthesis method allows for greater control over ZIF-8 membrane microstructure like thickness and grain boundaries. However the additional step of coating a strongly anchored seed layer on the support surface is essential before well inter-grown membranes.

Strong attachment of seed crystals to the substrate is difficult because of unfavorable heterogeneous nucleation. In addition, this makes the synthesis time-consuming and more complicated. Even though the MW-assisted seeding technique discussed in the previous chapter enabled strong attachment of seed crystals, still secondary growth was required to achieve ZIF-8 membranes with excellent performance. If it becomes possible to obtain well inter-grown films and membranes after just the seeding step, the synthesis time can be significantly reduced (~ 2 minutes) and simplified. However, to the best of our knowledge, no group has been able to achieve well inter-grown ZIF-8 membranes showing good propylene/propane separation performance in a simple, two-minute single step approach.

Here, we present the results from a systematic investigation to test if well inter-grown ZIF-8 membranes can be synthesized by this “one-pot” approach. The

desirable microstructure of the films was first identified following which, efforts were taken to develop a potential recipe for growing films reproducibly. Different zinc salts were used as the metal source in the seeding precursor solutions to try to obtain continuous ZIF-8 membranes. The one-pot membranes were investigated by X-ray diffraction, scanning electron micrograph images and binary gas performance measurements using the Agilent 7890A GC.

5.2 Experimental Section

5.2.1 Chemicals and Preparation of α-Al_2O_3 Supports

Chemicals were used as purchased without further treatments and purification. Zinc nitrate hexahydrate ($Zn(NO_3)_2.6H_2O$, 98%, Sigma-Aldrich,), Zinc chloride anhydrous ($ZnCl_2$, 99.95%, Alfa Aesar) and Zinc acetate dehydrate ($Zn(CH_3COO)_2.2H_2O$, 97+%, Alfa Aesar) were used as metal sources. 2-methylimidazole (m-Im) ($C_4H_5N_2$, 97%, Sigma-Aldrich) was the ligand. Sodium formate (SF) (HCOONa, 99%, Sigma-Aldrich) was the deprotonating agent to speed up the reaction. Methanol (99.8%, Alfa Aesar) was used as the solvent for seeding solutions and DI water was the solvent for the secondary growth. The procedure highlighted in section 4.2.2 was adopted for preparing the alumina supports for growing ZIF-8 films.

5.2.2 Formation of Continuous ZIF-8 Films/Membranes

The metal precursor solution was prepared by dissolving 8 mmol of the different zinc salts in 40 ml of methanol while the ligand precursor solution had 31.5 mmol of m-Im and 1.8 mmol of SF in 30 ml of methanol. The polished, sonicated

and dried alumina supports were placed vertically (with polished face slightly downwards) in a Teflon holder and then soaked in the metal precursor solution for 1 hour. After this, the metal-saturated supports were immersed in the ligand precursor in a microwave-transparent glass tube and immediately subjected to microwave radiation (100W and 1.5 minutes, CEM Microwave). Following cooling down to room temperature for 30 minutes, the ZIF-8 films were washed in methanol under constant stirring for 24 hours to remove the excess precursor solutions from inside the supports by solvent exchange. The films were then dried in a convection oven at 60°C for 6 hours to remove the methanol.

5.2.3 Characterizations

The crystalline phases for the different ZIF-8 films were tested by X-ray diffraction using the Rigaku diffractometer mentioned in section 3.3. SEM images for the films were taken in order to observe the changes in morphology with crystal growth time using the JEOL instrument with the specifications in section 3.3. The gas separation performance of the ZIF-8 membranes for a 50:50 mixture of propylene/propane was tested using a Wicke-Kallenbach setup and Agilent gas chromatograph with the conditions and setup illustrated in section 3.3.

5.3 Results and Discussion

The concept of MW-assisted seeding was illustrated in Fig 10. The desired microstructure to obtain well inter-grown membranes after just the seeding step is presented in Fig 28.

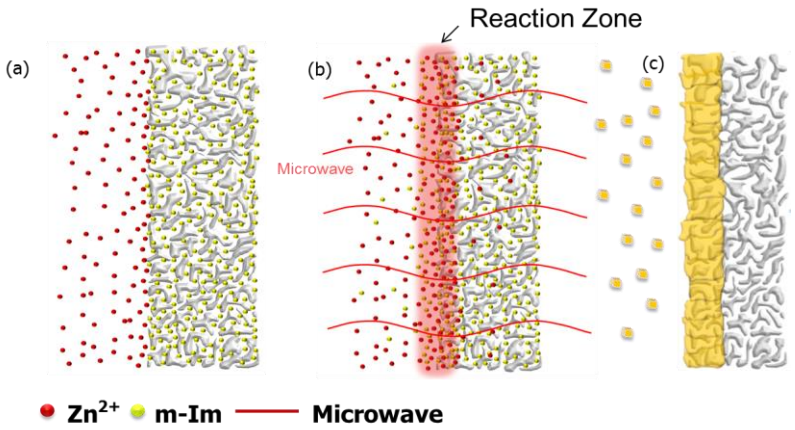

Fig 28: Schematic for the desired microstructure for one-pot synthesis technique

As mentioned in Chapter 4, the number, size and location of the seed crystals depend strongly on the rates of nucleation and solvation for the metal ions. The following rate of nucleation was empirically reported in [88]

$$Zn(NO_3)_2 > ZnCl_2 > Zn(CH_3COO)_2$$

Based on the Hofmeister anion effect, the following order for strength of solvation has been empirically estimated in [89]

$$Zn(CH_3COO)_2 > ZnCl_2 > Zn(NO_3)_2$$

5.3.1 Zinc Salt with the Desirable Microstructure

SEM images for the seed layers, ZIF-8 films/membranes (in this case), synthesized with different zinc salts as the metal sources were presented in Fig 13.

As can be seen from the SEM images, the morphologies and crystal sizes are widely different for the ZIF-8 films from different zinc salts. The illustrations reflect

the observed morphologies. The white part represents the alumina supports while the yellow part represents the ZIF-8 crystals and films.

As explained previously, higher rate of nucleation leads to smaller crystals and lower rate of nucleation leads to bigger crystals. Since zinc nitrate has the highest nucleation rate among the 3 zinc salts, crystals in the seed layer/films are smaller and more numerous as compared to zinc chloride and zinc acetate. For zinc acetate, the rate of nucleation is so slow that the ligand diffuses into the support by the time the reaction occurs under microwave radiation and the "reaction zone" is shifted inside the support. Thus, crystals are formed inside the supports predominantly. The acetate counter anions also have the strongest interaction with the solvents. While the zinc acetate films are being cooled down to room temperature (for 30 minutes following the seeding), some of the crystals formed on the support surface begin to grow, leading to inter-grown films being obtained. Zinc chloride shows intermediate properties between the two.

From the previous chapter, the microstructure of the membranes which showed good propylene/propane separation displayed the following characteristics:

- Good inter-growth
- Crystals inside the support (It was hypothesized in [36] that ZIF-8 membranes showed good selectivity because of crystals inside the support)

Out of all the ZIF-8 films/seed layers obtained, films from zinc acetate as the zinc source displayed both these characteristics. Thus, it can be concluded that ZIF-8 films synthesized by the MW-assisted seeding technique using zinc acetate as the metal source show potential for the "one-pot" approach.

5.3.2 Improvement in Separation Performance of ZIF-8 Films

When the ZIF-8 films synthesized using the recipe shown before with zinc acetate as the metal source were tested for gas performance measurement, they indicated defective morphologies. This was because the permeances for propylene were very high with almost no selectivity. Metal concentration in the precursor solution was doubled (M2X) to increase the crystals formed inside the support (characteristic for zinc acetate ZIF-8 films). This was expected to lower the permeance but improve the selectivity due to more crystals inside the support. However, there was no improvement in the performance for the ZIF-8 films grown.

It was hypothesized that probably 30 minutes for cooling down to room temperature was not sufficient for the zinc acetate crystals to grow into an inter-grown film. These macroscopic defects provide a resistance-free pathway for both propylene and propane, leading to large permeances and no separation. If crystals are allowed to grow for a longer time (60 minutes inside the CEM microwave instrument to slow down the rate of cooling), inter-growth might improve, thus healing the defects and improving the separation performance. This was confirmed by SEM images of the top view and binary gas performance measurements (Fig 29 and Table 12).

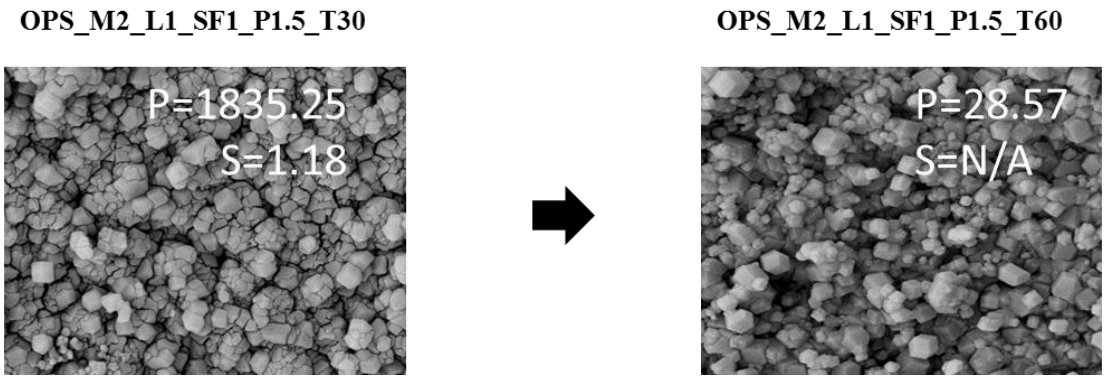

Fig 29: SEM images of the surface morphology change for the ZIF-8 films based on zinc acetate as the metal source

The base recipe for the synthesis (**M:L:SF** molar ratio of **1:4.65:2.96**) is indicated as **OPS_M1_L1_SF1_P1.5_T30,** where:

- OPS – One-Pot Synthesis
- M1 – Base recipe metal concentration
- L1 – Base recipe ligand concentration
- SF1 – Base recipe sodium formate concentration
- P1.5 – MW seeding time of 1.5 minutes
- T30 – Crystal growth time of 30 minutes

Table 12: C_3H_6/C_3H_8 binary gas performance of ZIF-8 films from zinc acetate

Membrane Serial #	**M:L:SF Ratio**	**Permeance ($\times 10^{-10}$ mol Pa^{-1} m^{-2} s^{-1})**		**Selectivity**
		Propylene (C_3H_6)	**Propane (C_3H_8)**	
OPS_M2_L1_SF1_P1.5_T30	1:2.33:1.48	**1835.25 ± 61.1**	1641.25 ± 38.78	**1.18 ± 0.02**
OPS_M2_L1_SF1_P1.5_T60*	1:2.33:1.48	**28.57**	N/A	**N/A**

* - Only one ZIF-8 film was synthesized per experiment because the cooling down was done inside the MW instrument

As can be seen from the SEM image and the binary gas permeation measurement, the surface defects for the zinc acetate ZIF-8 films are healed significantly, leading to lower permeances. However, there is no separation performance probably because the membrane cross-section is too thick due to doubling the metal concentration. It was hypothesized that enhancing the reaction rate by increasing the MW irradiation time during the seeding step would reduce the membrane thickness leading to greater permeances (Table 13).

Table 13: C_3H_6/C_3H_8 binary gas performance of ZIF-8 films with increased crystal growth time

Membrane Serial #	**M:L:SF Ratio**	**Permeance (x 10^{-10} mol Pa^{-1} m^{-2} s^{-1})**		**Selectivity**
		Propylene (C_3H_6)	**Propane (C_3H_8)**	
OPS_M2_L1_SF1_P1.5_T60*	1:2.33:1.48	**28.57**	N/A	**N/A**
OPS_M2_L1_SF1_P2_T60*	1:2.33:1.48	**196.09**	10.64	**18.43**
OPS_M2_L1_SF1_P2.5_T60*,a	1:2.33:1.48	**133.35**	2.18	**61.17**

* - Only one membrane was synthesized for the same reason as before

a –The temperature of the system reached closed to the boiling point of methanol (solvent), so the result cannot be trusted and this condition was not repeated again

It can be inferred from the above results that, for ZIF-8 films from zinc acetate

- Greater crystal growth time leads to better inter-growth
- Greater MW seeding time leads to higher permeance and better performance

Thus, the performance of ZIF-8 films as a function of different combinations of crystal growth times and MW seeding times was systematically investigated.

5.3.3 Reproducibility Issues

ZIF-8 films were synthesized from zinc acetate based recipe with the following conditions

- 3 different MW seeding times – 1.5, 1.75 and 2 minutes
- 2 different crystal growth times for each MW seeding time – 30 and 60 minutes

When this experiment was repeated twice, there were significant reproducibility issues. In other words, the performance of ZIF-8 films under one set of conditions during one experiment was completely different from the performance under the same conditions during another experiment. The following graphs illustrate the same (Fig 30).

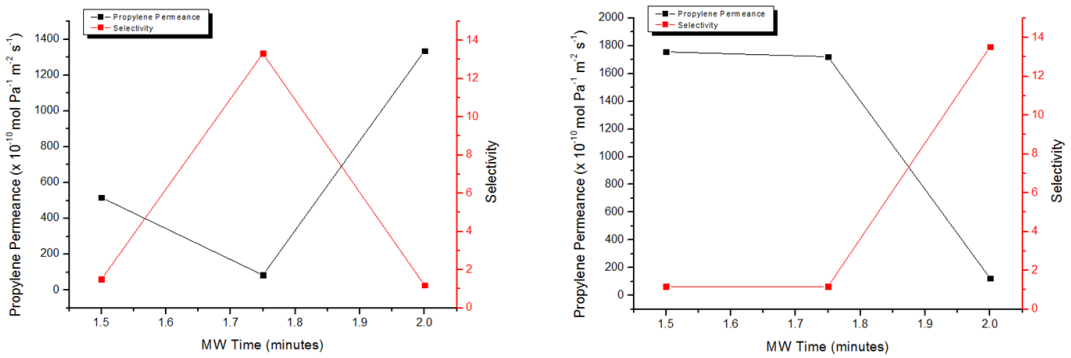

Fig 30: Week 1 and Week 2 results for membrane performance

To confirm that this was indeed a systematic error rather than typical experimental standard deviation, these experiments were repeated with the following modification – synthesized 1 membrane each with MW times of 1.5, 1.75 and 2 minutes for each day and repeated the experiment for several days. This systematic variability in results across different experiments continued to be present. Several potential causes for this variability were tested including

- Some leakage in the diffusion cell used for gas permeation measurement (Table 14)
- Loading of the sample into the diffusion cell (Table 15)
- Activation of the pores of the membranes (leading to lower permeances) (Table 16)
- Experimental error by me (Table 17)

Table 14: C_3H_6/C_3H_8 binary gas performance of ZIF-8 films tested using different diffusion cells

Membrane Serial #	**M:L:SF Ratio**	**Permeance ($\times 10^{-10}$ mol Pa^{-1} m^{-2} s^{-1})**		**Selectivity**
		Propylene (C_3H_6)	**Propane (C_3H_8)**	
OPS_M2_L1_SF1_P1.5_T30_UP_C1*	1:2.33:1.48	**608.11**	452.31	**1.34**
OPS_M2_L1_SF1_P1.5_T30_UP_C2*	1:2.33:1.48	**577.49**	427.35	**1.35**

* - UP – ZIF-8 films synthesized on unpolished supports

Table 15: C_3H_6/C_3H_8 binary gas performance of ZIF-8 films tested by lab mate

Membrane Serial #	**M:L:SF Ratio**	**Permeance (x 10^{-10} mol Pa^{-1} m^{-2} s^{-1})**		**Selectivity**
		Propylene (C_3H_6)	**Propane (C_3H_8)**	
OPS_M2_L1_SF1_P1.5_T30_UP_D1_Me	1 : 2.33 : 1.48	**15.53**	N/A	**N/A**
OPS_M2_L1_SF1_P1.5_T30_UP_D1_Lm	1 : 2.33 : 1.48	**20.91**	N/A	**N/A**
OPS_M2_L1_SF1_P1.5_T30_UP_D3_Me	1 : 2.33 : 1.48	**354.96**	269.58	**1.32**
OPS_M2_L1_SF1_P1.5_T30_UP_D3_Lm	1 : 2.33 : 1.48	**354.28**	266.11	**1.33**

* - D1 and D3 – ZIF-8 films synthesized on day 1 and day 3 respectively; Lm – Membranes tested by my lab mate

Table 16: C_3H_6/C_3H_8 binary gas performance of ZIF-8 films activated at 100°C

Membrane Serial #	**M:L:SF Ratio**	**Permeance (x 10^{-10} mol Pa^{-1} m^{-2} s^{-1})**		**Selectivity**
		Propylene (C_3H_6)	**Propane (C_3H_8)**	
OPS_M2_L1_SF1_P1.75_T30_UP_D1_Old	1 : 2.33 : 1.48	**17.26**	N/A	**N/A**
OPS_M2_L1_SF1_P1.75_T30_UP_D1_New	1 : 2.33 : 1.48	**27.63**	N/A	**N/A**

* - Old – ZIF-8 films before activation, and New – ZIF-8 films after activation at high temperature

Table 17: C_3H_6/C_3H_8 binary gas performance of ZIF-8 films synthesized by lab mate

Membrane Serial #	**M:L:SF Ratio**	**Permeance ($\times 10^{-10}$ mol Pa^{-1} m^{-2} s^{-1})**		**Selectivity**
		Propylene (C_3H_6)	**Propane (C_3H_8)**	
OPS_M2_L1_SF1_P1.5_T30_UP_D 1	1 : 2.33 : 1.48	**2046.48 ± 38.23**	1749.58 ± 35.16	**1.17**
OPS_M2_L1_SF1_P1.5_T30_UP_D 2	1 : 2.33 : 1.48	**71.26 ± 12.89**	1.08	**75.89**

From the above results, it was concluded that there was indeed some variation from experiments to experiments which was not due to random experimental error.

5.4 Conclusions

In conclusion, the potential for growing continuous ZIF-8 membranes with good propylene/propane separation performance by a simple, single step, 2 minute process was studied. Different zinc salts were used to synthesize ZIF-8 seed layers/films by the MW-assisted seeding technique. The ideal microstructure of having crystals inside the support (for good selectivity) and inter-grown films was found to be present for films from zinc acetate even after just the MW seeding step. This was due to the combination of slow nucleation and better crystal growth potential for the zinc acetate. By increasing the crystal growth time allowed from 30 minutes to 60 minutes, these ZIF-8 films/membranes showed good binary gas separation performance. However, it was very difficult to reproduce the results because the process was very sensitive to various factors. Several systematic

investigations were not able to identify what was the cause of this inherent reproducibility issue.

CHAPTER VI

EFFECT OF ACTIVATION TIME, AGING OF PRECURSOR SOLUTIONS, HIGH PRESSURE AND TEMPERATURE ON PERFORMANCE OF ZINC NITRATE ZIF-8 MEMBRANES BY SECONDARY GROWTH

6.1 Activation Time

Post synthesis solvent exchange time in methanol is referred here as activation time. According to the previously reported procedure followed [81], solvent exchange of the excess metal and ligand secondary growth solutions from inside the supports was performed for 5 days. Intuitively, this is much greater than the time necessary for effective removal of the excess precursors. As a result, reduction of this post-synthesis activation time will help to significantly reduce the total processing time for growing ZIF-8 membranes by secondary growth. To study the potential variation in the performance of ZIF-8 (zinc nitrate-based) membranes with the solvent exchange time in methanol, membranes were washed in methanol for 1 day, 3 days and 5 days before binary gas performance was tested (Table 18). Synthesis conditions and procedure was the same as reported in [81].

Table 18: C_3H_6/C_3H_8 binary gas performance of ZIF-8 membranes as a function of activation time

Activation Time	Permeance (x 10^{-10} mol Pa^{-1} m^{-2} s^{-1})		Selectivity
	Propylene (C_3H_6)	**Propane (C_3H_8)**	
1 day	**252.42**	9.07	**27.83**
3 days	**263.03**	9.7	**27.12**
5 days	**259.68**	9.14	**28.41**

As can be seen, though the membranes had relatively poor separation performance, there was not much change in the performance with activation time. As expected, the total time for processing can now be reduced without any loss in performance.

6.2 Aging of Precursor Solutions

In the ligand precursor solution for seeding, sodium formate plays the role of a deprotonating agent. Deprotonated ligands then react with the zinc ions in the saturated metal supports leading to formation of ZIF-8 seed layers. This process thus consists of the following equilibrium driven reaction

$$\boldsymbol{H - m - Im \rightleftharpoons H^{+} + m - Im^{-}}$$

When using freshly prepared precursor solutions, there is likely to be variations in the concentration of deprotonated ligands, leading to potential variability in results. Furthermore, the concentration of deprotonated ligands is a function of time and there might not be sufficient concentration of these ions

immediately after synthesis. An added advantage of making precursor solutions in bulk is that any variation in membrane microstructure and performance as a result of fresh batches of chemicals purchased can also be avoided.

Metal and ligand precursor solutions were prepared in bulk and used for the first time after 5 days of aging. Simultaneously, the effect of activation time was studied to ensure that membrane performance was stable as before with freshly prepared precursor solutions. Significant improvement in performance (selectivity increased almost 3 times) was achieved and is shown below (Table 19). With more practice, the separation performance of ZIF-8 membranes from zinc nitrate based recipe improved and reached the values shown in previous chapters.

Table 19: C_3H_6/C_3H_8 binary gas performance of ZIF-8 membranes from aged precursor solutions

Activation Time	**Permeance (x 10^{-10} mol Pa^{-1} m^{-2} s^{-1})**		**Selectivity**
	Propylene (C_3H_6)	**Propane (C_3H_8)**	
1 day	**234.08 ± 2.28**	3.84 ± 1.23	**60.98 ± 9.16**
3 days	**236.86 ± 7.89**	4.98 ± 1.43	**47.41 ± 8.64**
5 days	**231.29± 4.37**	4.03 ± 1.18	**57.63 ± 9.28**

6.3 Performance of ZIF-8 Membranes Under High Pressure

Though ZIF-8 membranes synthesized in this work showed good separation performance (separation factor ~ 100), the performance was measured at very mild conditions of 1 bar and room temperature. If these membranes are to be scaled up to

industrial production, their performance under typically harsher industrial conditions like higher pressures (at least 10 bar) and temperatures (~ 100°C) needs to be tested. As discussed in the background chapter, ZIF's exhibit the interesting phenomena of "gate-opening effect". This effect leads to an increase in pore sizes when larger gas molecules try to enter the apertures. It becomes possible in ZIF's as a direct consequence of the flapping motion of the ligands in the ZIF structure. Under higher feed-side pressures, this gate-opening effect is exaggerated leading to greater permeances for both propylene and propane. However, because the pore sizes are now increased, more propane molecules can enter the pores and this blocks the path for some propylene molecules. Thus, the increase in permeance is greater for propane than for propylene, leading to a reduction in selectivity with pressure. As the pressure is reduced again, the permeances drop and selectivites increase back again with very little loss in the original performance, provided the membranes are stable and do not undergo degradation at higher pressures. To test the performance of the ZIF-8 membranes synthesized under high pressure, one of the best membranes synthesized, was subjected to an increase in total feed pressure up to ~ 7 bar and then reduced back to 1 bar. The feed side pressure was controlled by use of a needle valve and pressure was monitored by a pressure gauge. After the pressure stabilized, measurements of the binary gas separation performance were performed. The Wicke-Kallenbach setup was modified for this high pressure measurement as shown below (Fig 31). The results are presented in Fig 32 and Table 20.

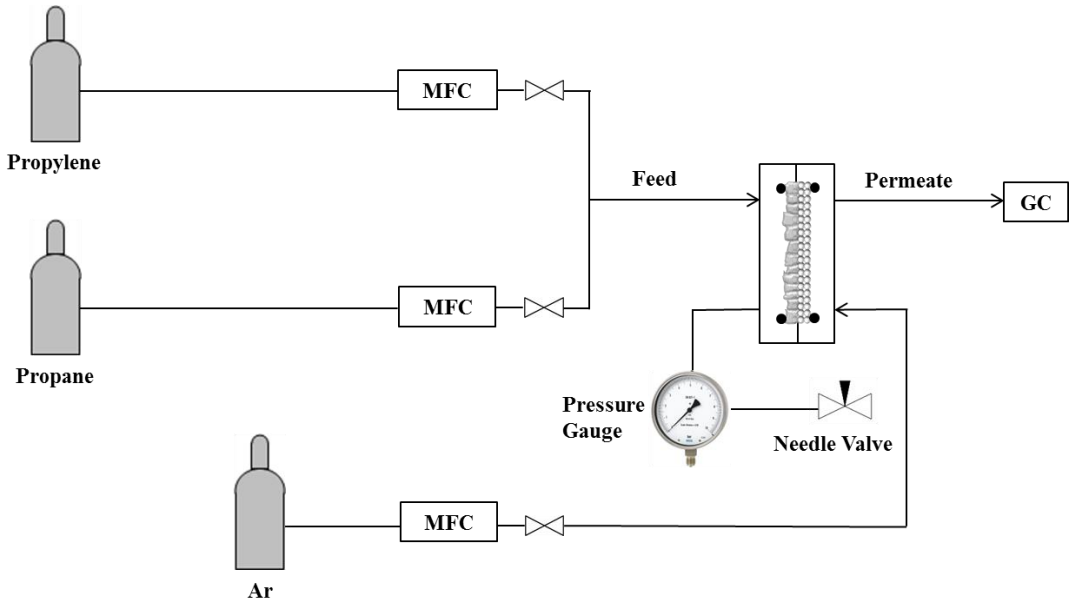

Fig 31: Setup used for the high pressure measurement

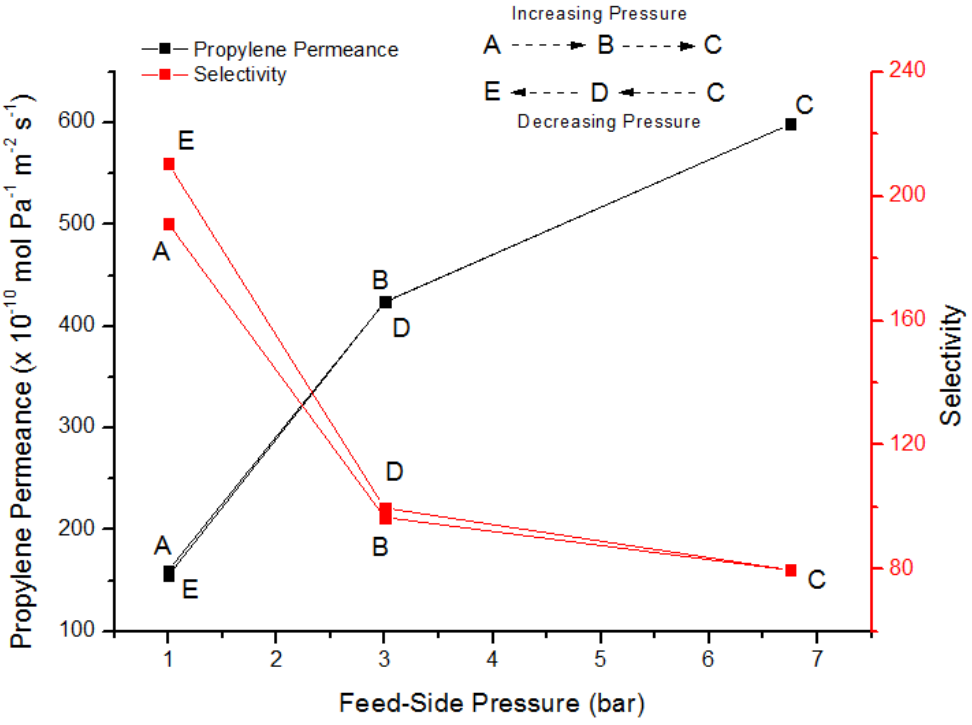

Fig 32: Variation of propylene permeance and selectivity as a function of feed-side pressure

Table 20: C_3H_6/C_3H_8 binary gas performance of high quality ZIF-8 membrane with pressure

Feed-Side Absolute Pressure (bar)	**Permeance (x 10^{-10} mol Pa^{-1} m^{-2} s^{-1})**		**Selectivity**
	Propylene (C_3H_6)	**Propane (C_3H_8)**	
1	**154.99**	0.81	**191.35**
3.8	**423.85**	4.38	**96.77**
6.75	**598.88**	7.51	**79.74**
3.8	**423.83**	4.25	**99.72**
1	**160.01**	0.76	**210.53**

As can be seen, the membrane performance remained stable during the depressurizing stage as well, which indicated that increase in permeances and loss in selectivity were due to "gate-opening" effect and not due to membrane degradation at high pressures.

6.4 Performance of ZIF-8 Membranes Under High Temperature

The high quality membrane tested under high pressure in the previous section was then tested at temperatures of 60°C and 120°C, at pressures of 1 bar and 6.75 bar. Heating tape was used to heat the feed side and diffusion cell to the said temperatures and temperature control was achieved using Thermolyne Heating Tape and Percentage Control. Temperatures were monitored using an Omega multi-channel thermocouple. The results are presented below (Fig 33 and Tables 21 and 22).

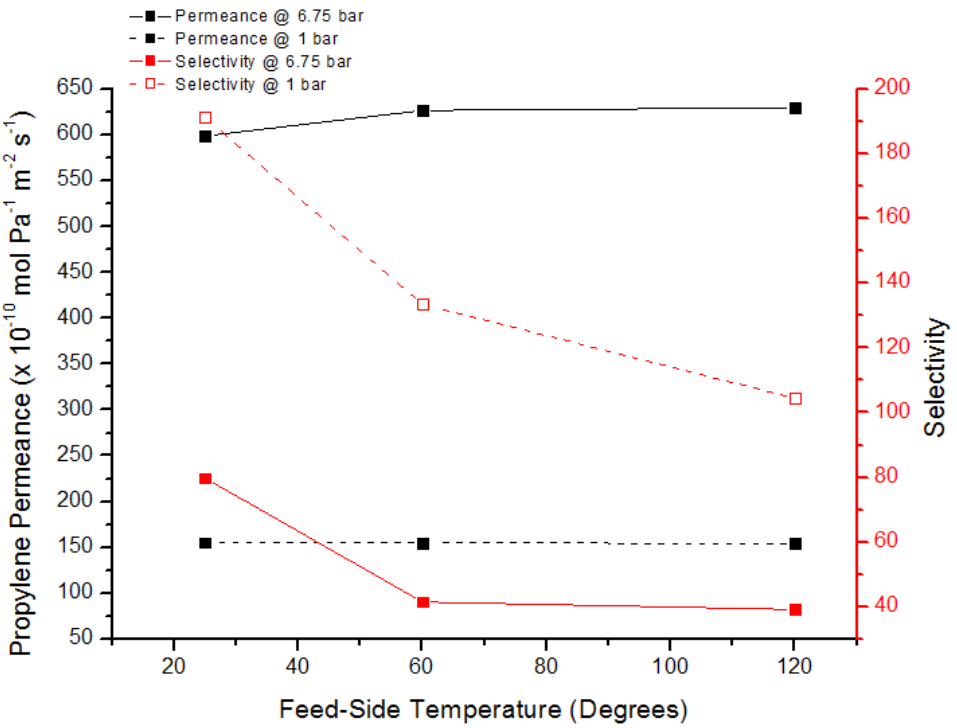

Fig 33: Variation of propylene permeance and selectivity as a function of feed-side temperature

Table 21: C_3H_6/C_3H_8 binary gas performance of high quality ZIF-8 membrane with temperature (pressure of 1 bar)

Feed-Side Temperature (°C)	**Permeance (x 10^{-10} mol Pa^{-1} m^{-2} s^{-1})**		**Selectivity**
	Propylene (C_3H_6)	**Propane (C_3H_8)**	
Room Temperature	**154.99**	0.81	**191.35**
60	**154.8**	1.16	**133.45**
120	**154.57**	1.48	**104.44**

Table 22: C_3H_6/C_3H_8 binary gas performance of high quality ZIF-8 membrane with temperature (pressure of 6.75 bar)

Feed-Side Temperature (°C)	**Permeance (x 10^{-10} mol Pa^{-1} m^{-2} s^{-1})**		**Selectivity**
	Propylene (C_3H_6)	**Propane (C_3H_8)**	
Room Temperature	**598.88**	7.51	**79.74**
60	**626.87**	15.13	**41.43**
120	**629.9**	16.12	**39.08**

The exact mechanism for how propane permeance increases without any significant change in propylene permeance is still not known. However, it is hypothesized that possibly the sticking coefficient (which deals with the probability of gas molecule adsorbing on the membrane's pore entrances when it strikes the surface) for propane was somehow enhanced. This led to increase in propane permeances, leading to a decrease in selectivity. However, the possibility of increase in effective pore size at higher temperatures cannot be completely neglected. Whatever the mechanism, even under high pressure and high temperature, the ZIF-8 membrane showed good propylene/propane separation performance and shows promise for industrial application.

6.5 Conclusions

The stability of membrane performance was studied under different process conditions like post synthesis activation (methanol washing) time, aging of seed precursor solutions, high pressure and high temperature. The post synthesis

activation time was not found to have any impact on membrane performance and thus the total processing time can now be significantly reduced (by 4 days). Aging of seed precursor solutions was found to significantly enhance membrane performance (selectivity increased by 3 times) and improve reproducibility. Even under high feed-side pressure operation (~ 7 bar), the ZIF-8 membrane tested was shown to be stable and did not undergo degradation. However, there was increase in permeances and a reduction in selectivity due to "gate opening" effect at these higher pressures. The performance of the membrane was also tested at temperatures of 60°C and 120°C under high pressure to try to simulate harsher industrial conditions. The membrane had good separation performance even under these conditions.

CHAPTER VII

CONCLUSIONS AND FUTURE WORK

7.1 Conclusions

Systematic studies of several different parameters like zinc salt effect, potential for one-step synthesis, activation time, aging of precursor solutions and high pressure, high temperature on the performance of ZIF-8 membranes was carried out in this thesis.

In Chapter IV, a systematic study on the effect of different zinc salts on the seed layer morphology and consequently membrane performance. ZIF-8 seed layers and membranes synthesized from different zinc salts had different morphologies and performances due to different rates of nucleation and crystal growth for each zinc salt. For the MW-assisted seeding technique followed by secondary growth, it was determined that zinc nitrate seed layers (densely packed with uniform small crystals) had the best morphology for membrane growth in the aqueous secondary growth step. This was potentially due to ability to form membranes with excellent grain boundaries following secondary growth. The effect of different zinc salts, with different crystal growth rates, on the secondary growth step was subsequently investigated. It was concluded that, for zinc nitrate seed layers, rate of crystal growth should ideally be higher to form membranes showing good performances (permeances ~ 200 mol Pa^{-1} m^{-2} s^{-1} and selectivity ~ 100). When 50:50 mixtures (by concentration) of different zinc salts were used in both the seed layers and secondary growth step, average properties for seed layer morphology, membrane thickness and grain boundaries were observed.

In Chapter V, the potential for growing continuous ZIF-8 membranes with good propylene/propane separation performance by a simple, single step, 2 minute process was studied. Different zinc salts were used to synthesize ZIF-8 seed layers/films by the MW-assisted seeding technique. The ideal microstructure of having crystals inside the support (for good selectivity) and inter-grown films was found to be present for films from zinc acetate even after just the MW seeding step. This was due to the combination of slow nucleation and better crystal growth potential for the zinc acetate. By increasing the crystal growth time allowed from 30 minutes to 60 minutes, these ZIF-8 films/membranes showed good binary gas separation performance. However, it was very difficult to reproduce the results because the process was very sensitive to various factors.

In Chapter VI, the stability of membrane performance under different process conditions like post synthesis activation (methanol washing) time, aging of seed precursor solutions, high pressure and high temperature was tested. The post synthesis activation time was not found to have any impact on membrane performance and thus the total processing time can now be significantly reduced (by 4 days). Aging of seed precursor solutions was found to significantly enhance membrane performance (selectivity increased by 3 times) and improve reproducibility. Even under high feed-side pressure operation (~ 7 bar), the ZIF-8 membrane tested was shown to be stable and did not undergo degradation. However, there was increase in permeances and a reduction in selectivity due to “gate opening” effect at these higher pressures. The membrane was also tested at temperatures of 60°C and 120°C under high pressure and shown to have good separation performance even under these harsh conditions.

7.2 Future Work

One-pot synthesis of ZIF-8 membranes shows great potential for a simple and reproducible synthesis technique that can be scaled up for industrial applications. However, detailed investigations to overcome the reproducibility issues are necessary to start on this exciting path.

Testing the performance of high quality ZIF-8 membranes under even harsher conditions of pressure and temperature will help to identify the current operating limits for them. This knowledge is extremely useful if these membranes are indeed to be applied on a large scale in industry. However, setup for such a high pressure, high temperature measurement must be very robust and efficient and needs to be designed. The separation capability of our ZIF-8 membranes for liquid hydrocarbon separations like the butane isomers, xylene isomers, etc. also is of interest.

REFERENCES

1. DF Sanders, ZP Smith, R Guo, LM Robeson, JE McGrath, DR Paul, BD Freeman.; *Polymer*, 2013, **54**, 4729-4761
2. S Robinson, R Jubin, B Choate, P Angelini, T Armstrong, R Counce, W Griffith, T Klasson, G Muralidharan, C Narula, V Sikka, G Closset, G Keller, J Watson.; *US Department of Energy Report*, 2004
3. KB Lee, MG Beaver, HS Caram, S Sircar.; *Ind. Eng. Chem. Res.*, 2008, **47**, 8048-8062
4. D Aaron, C Tsouris.; *Sep. Sci. Technol.*, 2005, **40**, 321-348
5. JD Figueroa, T Fout, S Plasynski, H McIlvried, RD Srivastava.; *International Journal of Greenhouse Gas Control*, 2008, **2**, 9-20
6. K Scoth.; *Handbook of Industrial Membranes, Elsevier*, **2nd ed**, 1999
7. MT Ravanchi, T Kaghazchi, A Kargari.; *Desalination*, 2009, **235**, 199-244
8. RW Baker.; *Ind. Eng. Chem. Res.*, 2002, **41**, 1393-1411
9. RW Baker, K Lokhandwala.; *Ind. Eng. Chem. Res.*, 2008, **47**, 2109-2121
10. RW Baker.; *Membrane Technology and Applications, John Wiley & Sons, Ltd*, 2004
11. P Bernardo and E Drioli.; *Petroleum Chemistry*, 2010, **50**, 271-282
12. R Spillman.; *Chem. Eng. Prog.*, 1989, **41**, 85
13. R Prasad, RL Shaner, KJ Doshi.; *Polymeric gas separation membranes, Boca Raton CRC Press*, 1994
14. P Bernardo, E Drioli, G Golemme.; *Ind. Eng. Chem. Res.*, 2009, **48**, 4638-4663

15. RL Burns, WJ Koros.; *J. Membr. Sci.*, 2003, **211**, 299-309
16. ML Chng, Y Xiao, T-S Chung, M Toriida, S Tamai.; *Carbon*, 2009, **47**, 1857-1866
17. K-I Okamoto, S Kawamura, M Yoshino, H Kita, Y Hirayama, N Tanihara, Y Kusuki.; *Ind. Eng. Chem. Res.*, 1999, **38**, 4424-4432
18. J-I Hayashi, H Mizuta, M Yamamoto, K Kusakabe, S Morooka, S-H Suh.; *Ind. Eng. Chem. Res.*, 1996, **35**, 4176-4181
19. C Zhang, Y Dai, JR Johnson, O Karvan, WJ Koros.; *J. Membr. Sci.*, 2012, **389**, 34-42
20. IG Giannakopoulos, V Nikolakis.; *Ind. Eng. Chem. Res.*, 2005, **46**, 226-230
21. E Koresh, A Soffer.; *Sep. Sci. Technol.*, 1983, **18**, 723-734
22. CW Jones, WJ Koros.; *Carbon*, 1994, **32**, 1419-1425
23. H Hatori, Y Yamada, M Shiraishi, H Nakata, S Yoshitomi.; *Carbon*, 1992, **30**, 305-306
24. H Suda, K Haraya.; *J. Chem. Soc., Chem. Commun.*, 1995, **11**, 1179-1180
25. W Shusen, Z Meiyun, W Zhizhong.; *J. Membr. Sci.*, 1996, **109**, 267-270
26. J Hayashi, H Mizuta, M Yamamoto, K Kusakabe, S Morooka.; *J. Membr. Sci.*, 1997, **124**, 243-251
27. MB Shiflett, HC Foley.; *Science*, 1999, **285**, 1902-1905
28. C Liu, S Kulprathipanja, S Wilson.; *U.S. Patent Appl. 2007/0209505 A1*, 2007
29. IG Giannakopoulos, V Nikolakis.; *J. Membr. Sci.*, 2007, **305**, 332-337
30. AS Kovvali, KK Sirkar.; *Ind. Eng. Chem. Res.*, 2001, **40**, 2502-2511

31. JD Way, RD Noble, DL Reed, GM Ginley, LA Jan.; *AIChE J.*, 1987, **33**, 480-487
32. T-J Kim, B Li, MB Ha¨gg.; *J. Polym. Sci., Part B: Polym. Phys.*, 2004, **42**, 4326-4336
33. SW Kang, JH Kim, K Char, J Won, YS Kang.; *J. Membr. Sci.*, 2006, **285**, 102-107
34. T Merkel, R Blanc, J Zeid, A Suwarlim, B Firat, H Wijmans, M Asaro, M Greene.; *US Department of Energy Report*, 2007
35. TT Moore, WJ Koros.; *J. Mol. Struct.*, 2005, **739**, 87-98
36. HT Kwon, HK Jeong.; *J. Am. Chem. Soc.*, 2013, **135**, 10763-10768
37. EE McLeary, JC Jansen, F Kapteijn.; *Microporous Mesoporous Mater.*, 2006, **90**, 198-220
38. E Haldoupis, S Nair, DS Sholl.; *J. Am. Chem. Soc.*, 2010, **132**, 7528-7539
39. JR Li, RJ Kuppler, HC Zhou.; *Chem. Soc. Rev.*, 2009, **38**, 1477-1504
40. LJ Murray, M Dinca, JR Long.; *Chem. Soc. Rev.*, 2009, **38**, 1294-1314
41. H Patricia, S Christian, G David, BE Cedric, P Sandrine, S Clement, G Ferey.; *Adv. Mater.*, 2009, **21**, 1931-1935
42. MD Allendorf, RJT Houk, L Andruszkiewicz, AA Talin, J Pikarsky, A Choudhury, KA Gall, PJ Hesketh.; *J. Am. Chem. Soc.*, 2008, **130**, 14404-14405
43. A Alshammari, Z Jiang, KE Cordova.; *Metal Organic Frameworks as Emerging Photocatalysts, Semiconductor Photocatalysis - Materials, Mechanisms and Applications, InTech*, 2016

44. Y-S Li, HG Bux, A Feldhoff, G-L Li, WS Yang, J Caro.; *Adv. Mater.*, 2010, **22**, 3322-3326
45. HG Bux, FY Liang, Y-S Li, J Cravillon, M Wiebcke, J Caro.; *J. Am. Chem. Soc.*, 2009, **131**, 16000-16001
46. Y-S Li, FY Liang, HG Bux, A Feldhoff, WS Yang, J Caro.; *Angew. Chem., Int. Ed.*, 2010, **49**, 548-551
47. SR Venna, MA Carreon.; *J. Am. Chem. Soc.*, 2010, **132**, 76-78
48. Y Liu, E Hu, EA Khan, Z Lai.; *J. Membr. Sci.*, 2010, **353**, 36-40
49. A Huang, HG Bux, F Steinbach, J Caro.; *Angew. Chem., Int. Ed.*, 2010, **122**, 5078-5081
50. MC McCarthy, VV Guerrero, G Barnett, HK Jeong.; *Langmuir*, 2010, **26**, 14636-14641
51. KS Park, Z Ni, AP Cote, JY Choi, RD Huang, FJ Uribe-Romo, HK Chae, M O'Keeffe, OM Yaghi.; *Proc. Natl. Acad. Sci. U.S.A.*, 2006, **103**, 10186-10191
52. D Fairen-Jimenez, SA Moggach, MT Wharmby, PA Wright, S Parsons, T Deuren.; *J. Am. Chem. Soc.*, 2011, **133**, 8900-8902
53. HT Kwon, HK Jeong, AS Lee, HS An, JS Lee.; *J. Am. Chem. Soc*., 2015, **137**, 12304-12311
54. RJ Pearson.; *J. Am. Chem. Soc.*, 1963, **85**, 3533-3539
55. OM Yaghi, G Li, H Li.; *Nature*, 1995, **378**, 703-706
56. N Stock, S Biswas.; *Chem. Rev.*, 2012, **112**, 933-969
57. A Rabenau.; *Angew. Chem., Int. Ed. Engl.*, 1985, **24**, 1026-1040
58. BF Hoskins, RJ Robson.; *J. Am. Chem. Soc.*, 1990, **112**, 1546-1554
59. S Keskin, S Kizilel.; *Ind. Eng. Chem. Res.*, 2011, **50**, 1799-1812

60. U Mueller, H Puetter, M Hesse, H Wessel.; *U.S. Patent Appl. 2005/049892*, 2005

61. A Lazuen-Garay, A Pichon, SL James.; *Chem. Soc. Rev.*, 2007, **36**, 846-855

62. AJ Burgraff, L Cot.; *Fundamentals of Inorganic Membrane Science and Technology*, **Vol 4**, *Elsevier*, 1996

63. Y Yoo, HK Jeong.; *Chem. Commun.*, 2008, **21**, 2441-2443

64. R Ranjan, M Tsapatsis.; *Chem. Mater.*, 2009, **21**, 4920-4924

65. Y Yoo, ZP Lai, HK Jeong.; *Microporous Mesoporous Mater.*, 2009, **123**, 100-106

66. VV Guerrero, Y Yoo, MC McCarthy, HK Jeong.; *J. Mater. Chem.*, 2010, **20**, 3938-3943

67. A Huang, W Dou, J Caro.; *J. Am. Chem. Soc.*, 2010, **132**, 15562-15564

68. JG Nguyen, SM Cohen.; *J. Am. Chem. Soc.*, 2010, **132**, 4560-4561

69. O Shekhah, J Liu, RA Fischer, C Woll.; *Chem. Soc. Rev.*, 2011, **40**, 1081-1106

70. E Biemmi, C Scherb, T Bein.; *J. Am. Chem. Soc.*, 2007, **129**, 8054-8055

71. D Zacher, A Baunemann, S Hermes, RA Fischer.; *J. Mater. Chem.*, 2007, **17**, 2785-2792

72. P Horcajada, C Serre, D Grosso, C Boissiere, S Perruchas, C Sanchez, G Ferey.; *Adv. Mater.*, 2009, **21**, 1931-1935

73. R Ameloot, L Stappers, J Fransaer, L Alaerts, BF Sels, DE de-Vos.; *Chem. Mater.*, 2009, **21**, 2580-2582

74. R Ameloot, E Gobechiya, H-I Uji, JA Martens, J Hofkens, L Alaerts, BF Sels, DE de-Vos.; *Adv. Mater.*, 2010, **22**, 2685-2688

75. Schoedel, C Scherb, T Bein.; *Angew. Chem., Int. Ed.*, 2010, **49**, 7225-7228
76. O Shekhah, H Wang, S Kowarik, F Schreiber, M Paulus, M Tolan, C Sternemann, F Evers, D Zacher, RA Fischer, C Woll.; *J. Am. Chem. Soc.*, 2007, **129**, 15118-15119
77. GR Gavalas.; *Materials Science of Membranes for Gas and Vapor Separation, John Wiley & Sons, Ltd*, 2006, 307-336
78. MC Lovallo, A Gouzinis, M Tsapatsis.; *Aiche J.*, 1998, **44**, 1903-1913
79. MA Snyder, M Tsapatsis.; *Angew. Chem., Int. Ed.*, 2007, **46**, 7560-7573
80. Y Hu, X Dong, J Nan, W Jin, X Ren, N Xu, YM Lee.; *Chem. Comm.*, 2011, **47**, 737-739
81. HT Kwon, HK Jeong.; *Chem. Comm.*, 2013, **49**, 3854-3856
82. BL Hayes.; *Microwave Synthesis – Chemistry at the Speed of Light, CEM Publishing*, 2002
83. NA Khan, SH Jhung.; *Coordination Chemistry Reviews*, 2015, **285**, 11-23
84. KH Li, DH Olson, J Seidel, TJ Emge, HW Gong, H P Zeng, J Li.; *J. Am. Chem. Soc.*, 2009, **131**, 10368-10369
85. Y Pan, Z Lai.; *Chem. Comm.*, 2011, **47**, 10275-10277
86. RM Barrer.; *J. Chem. Soc.*, 1990, **86**, 1123-1130
87. R de Lange, K Keizer, A Burggraaf.; *J. Membr. Sci.*, 1995, **104**, 81-100
88. A Schejn, L Balan, V Falk, L Aranda, G Medjahdi, R Schneider.; *Cryst. Eng. Comm.*, 2014, **16**, 4493-4500
89. B Chen, F Bai, Y Zhu, Y Xia.; *RSC Adv.*, 2014, **4**, 47421-47428